

**APPLICATION OF POLYMER FLOODING IN
SANDSTONE RESERVOIRS OF UZEN FIELD**

by

ILYAS BEKPAYEV

2021

Thesis submitted to the School of Mining and Geosciences of Nazarbayev
University in Partial Fulfillment of the Requirements for the Degree of
Master of Science in Petroleum Engineering

Nazarbayev University
2021

Acknowledgements

I would like to express my gratitude to my supervisor Professor Muhammad Rehan Hashmet for helping me to find an interesting and important topic and for useful and valuable guidance and during the whole study. I would also like to sincerely thank my co-supervisor Professor Peyman Pourafshary for his excellent suggestions and recommendations.

Taking this opportunity, I would like to thank all my groupmates and all Professors and staff of the Department of Petroleum Engineering at Nazarbayev University for creating a fruitful atmosphere for development.

My sincere thanks to my family, which have supported me throughout the whole period of study at Nazarbayev University.

Originality Statement

I, Ilyas Bekpayev, hereby declare that this submission is my own work and to the best of my knowledge it contains no materials previously published or written by another person, or substantial proportions of material which have been accepted for the award of any other degree or diploma at Nazarbayev University or any other educational institution, except where due acknowledgement is made in the thesis.

Any contribution made to the research by others, with whom I have worked at NU or elsewhere is explicitly acknowledged in the thesis.

I also declare that the intellectual content of this thesis is the product of my own work, except to the extent that assistance from others in the project's design and conception or in style, presentation and linguistic expression is acknowledged.

Signed on 03.04.2020.

ABSTRACT

One of the most applied Chemical Enhanced Oil Recovery (CEOR) techniques is polymer flooding, which uses polymer solutions to increase the viscosity of the displacing water and enhance mobility control and sweep efficiency. Polymer flooding can be applied in mature oilfields, which already undergo secondary recovery with a gradual decrease in production. One such reservoir is the Uzen field, which is located in the western part of Kazakhstan. The Uzen field is one of the largest and oldest oilfields in the whole country and an increase in its oil production might be crucial to satisfy growing energy demand. A successful application of polymer flooding in a certain field requires a proper polymer selection followed by a well-planned and sophisticated assessment of its performance under reservoir conditions. This work is focused on the lab scale evaluation of three synthetic polymers performance in conditions of the Uzen field. The investigated polymers are co-polymers with functional groups of acrylamides (AM), Acrylamido-Tert-Butyl-Sulfonate (ATBS). Sav 10, Sav 19, and Sav 10 XV polymers. The work sequence:

- Investigation of polymer concentration and temperature effects on rheological behavior of polymers
- Mechanical stability under high shear rate
- Evaluation of long-term thermal stability of polymers
- Injectivity tests for the evaluation of permeability and mobility reduction due to polymers flooding at the core scale and required differential pressure for the injection.
- Investigation of displacement efficiency of one the most suitable candidate at the core scale.

Sav 10 polymer showed the best mechanical stability with the viscosity retention of 50 % after 10 minutes exposure to high shear rate. All candidates were able retain at least 50% of their initial viscosities after 2 months at 60 °C. The injection of Sav 10 polymer provided the best injectivity with the lowest differential pressures and permeability reduction. The application of Sav 10 flooding was effective and increased the cumulative oil recovery by 12 % after the brine flooding. To conclude, the polymer flooding with Sav 10 polymer in the conditions of the Uzen field was effective EOR technique and can be recommended for the implementation.

Table of content

| | |
|--|--|
| List of Figures | 6 |
| List of Tables | 10 |
| Abbreviations and symbols..... | 11 |
| 1. Introduction..... | 12 |
| 1.1. Background..... | 12 |
| 1.2. Literature review | 16 |
| 1.2.1. The Uzen field characteristics..... | 16 |
| 1.2.2. Reservoir screening criteria for the application of polymer flooding..... | 21 |
| 1.2.3. Polymer Stability | 22 |
| 1.2.4.1. Mechanical stability..... | 22 |
| 1.2.4.2. Chemical stability | 25 |
| 1.2.4.3. Thermal stability | 29 |
| 1.2.4.4. Biological degradation..... | 31 |
| 1.2.5. Overview of polymers for the application in the Uzen field | 33 |
| 1.2.5.1. Zetag 8187G (Firozjahi et al., 2019)..... | 33 |
| 1.2.5.2. Combination of SAV37 and AN125VHM (Firozjahi et al., 2019) | 36 |
| 1.2.5.3. The bulk scale investigation of 9 synthetic ATBS and NVP containing polymers. | 39 |
| 1.2.5.4. Comparative analysis of polymer flooding using polysaccharides and a synthetic polymer under harsh conditions (Liang et al., 2019)..... | 42 |
| 1.3. Problem definition | Ошибка! Закладка не определена. |
| 1.4. Thesis objectives..... | Ошибка! Закладка не определена. |
| 2. Methodology | 47 |
| 2.1. Materials | 48 |
| 2.1.1. Formation water:..... | 48 |

| | |
|---|----|
| 2.1.2. Oil sample | 49 |
| 2.1.3. Rock sample..... | 50 |
| 2.1.4. Polymers | 50 |
| 2.2. Experimental methods and procedure..... | 51 |
| 2.2.1. Brine and polymer solutions preparation procedure..... | 51 |
| 2.2.2. Bulk scale rheological investigation | 52 |
| 2.2.3. Long-term thermal stability tests | 53 |
| 2.2.4. Mechanical degradation | 53 |
| 2.2.5. Core preparation..... | 54 |
| 2.2.6. Injectivity tests | 54 |
| 2.2.7. Oil Displacement test..... | 56 |
| 3. Results..... | 58 |
| 3.1. Bulk scale rheological investigation | 58 |
| 3.1.1. The effect of concentration. | 58 |
| 3.1.2. The effect of temperature..... | 60 |
| 3.2. Mechanical stability | 63 |
| 3.3. Long-term thermal stability test..... | 65 |
| 3.4. Injectivity tests..... | 66 |
| 3.5. Oil displacement test..... | 69 |
| 4. Conclusions and Recommendations | 72 |
| 6. REFERENCES | 74 |

List of Figures

| | |
|--|----|
| Figure 1 - Structural sections of the Uzen field with hydrocarbon distribution: a) - along the fold axis; b) - perpendicular to the fold axis (Ulmishek, 1990) | 17 |
| Figure 2 - Production History of the Uzen Filed for 1965-2008 (C & C Reservoirs, 2010) | 19 |
| Figure 3 - Dynamics of the main technological production indicators of oil-bearing horizons in the Uzen field for 2009 - 1 st half of 2014 | 19 |
| Figure 4 - Viscosity - shear rate relationship of polymer solutions (Green and Willhite 1998)... | 23 |
| Figure 5 - Viscosity loss of a xanthan solution with increase of shear rate in Berea sandstone core; not significant influence was detected (Seright et al., 1983). | 24 |
| Figure 6 - Viscosity loss of a HPAM samples (unsheared and presheared) with increase of shear rate in Berea sandstone core; not significant influence was detected (Seright et al., 1983). | 24 |
| Figure 7 - Influence of oxygen effect on HPAM stability at 90°C combined with three different level of oxygen: 1, low level of oxygen; 2, air; 3, oxygen. Source (Luo et al., 2006). | 26 |
| Figure 8: a - Effect of Effect of NaCl concentration on viscosity of HPAM polymer; b - Effect of CaCl ₂ concentration on viscosity of HPAM polymer..... | 27 |
| Figure 9 - HPAM viscosity alteration by presence of dissolved oxygen and Fe ²⁺ at 90°C (Seright and Skjevrak, 2014). | 28 |
| Figure 10 - HPAM-ATBS viscosity alteration by presence of dissolved oxygen and Fe ²⁺ at 90°C (Seright and Skjevrak, 2014). | 28 |
| Figure 11 - Effect of Fe ²⁺ , temperature, and salinity on HPAM-ATBS stability (Seright and Skjevrak, 2014). | 28 |
| Figure 12 - Effect of temperature on apparent viscosity of HPAM-based polymer with ATBS monomer in the functional structure (Wu, 2016)..... | 30 |
| Figure 13 - Difference between gradual temperatre increase and a effect of constant temperature (Tan, 1998)..... | 30 |
| Figure 14 - Bacterial degradation of polymer solution (Niu et al., 2006). | 31 |
| Figure 15 - Polymer viscosity alteration due to different level of salinity in high temperature condition | 34 |

| | |
|---|----|
| Figure 16 - Polymer viscosity alteration due to different level variation of temperature in 150,000 ppm salinity..... | 34 |
| Figure 17 – Long-term polymer stability of Zetag 8187G (2000 ppm of polymer solution, temperature of 86 °C, and salinity level of 150,000 ppm,)..... | 35 |
| Figure 18 - Pore Volume Injected vs. Oil recovery factor for water and polymer flooding | 36 |
| Figure 19 - Residual oil saturation vs. Pore Volume Injected for water and polymer flooding ... | 36 |
| Figure 20 - Effect of increasing temperature on viscosity of 6000 ppm of polymer solution with different weight percentages of two SAV37 and AN125VHM polymer (Salinity of 10000 ppm). | 37 |
| Figure 21 - Effect of increasing salinity on viscosity of 6000 ppm of polymer solution with different weight percentages of two SAV37 and AN125VHM polymer (Room temperature).... | 37 |
| Figure 22- Thermal stability of polymer solutions in salinity in salinity of 150000 ppm | 38 |
| Figure 23 - Oil recovery factor vs. PV injected curves for two flooding regimes (confining pressure – 2000 psi, temperature – 85 °C, salinity level – 10000 ppm) | 39 |
| Figure 24 - Oil saturation vs PV injected curves for two flooding regimes(confining pressure – 2000 psi, temperature – 85 °C, salinity level – 10000 ppm) | 39 |
| Figure 25 - Long-term thermal stability polymers from low to medium level of ATBS content at the salinity level of 98000 ppm and polymer concentration of 1500 ppm | 40 |
| Figure 26 - Long-term thermal stability of polymers at the salinity level of 56000 ppm and polymer concentration of 1500 ppm | 41 |
| Figure 27 - Long-term thermal stability of polymers at the salinity level of 98000 ppm and polymer concentration of 1500 ppm (Sav226 – 2000 ppm)..... | 41 |
| Figure 28 - The guidance of polymer selection based on salinity and temperature. | 41 |
| Figure 29 – The chemical structures of investigated polymers | 42 |
| Figure 30 - Loss of apparent viscosity with increasing temperature (no salt, shear rate = 100 s ⁻¹). | 43 |
| Figure 31 - Loss of apparent viscosity and viscosity retention with increasing level of salinity (temperature = 85 °C, shear rate = 100 s ⁻¹)..... | 43 |
| Figure 32 - Viscosity of polymer vs. concentration (temperature = 85 °C; salinity level – 10.1 × 10 ⁴ mg/L)..... | 44 |

| | |
|--|----|
| Figure 33 - Long term thermal stability test in salinity of 10.1×10^4 mg/L..... | 44 |
| Figure 34 – Viscous modulus (G'') and dynamic elastic modulus (G') for the polymer solution (temperature = 85 °C; salinity level – 10.1×10^4 mg/L). | 45 |
| Figure 35 - Pressure drop and Recovery factor vs. Injected PV (temperature = 85 °C; salinity level – 10.1×10^4 mg/L) (A, b, c, d is for Diutan gum, Scleroglucan, Xanthan gum and HPAM respectively)..... | 46 |
| Figure 36 - Flowchart of polymer screening process..... | 48 |
| Figure 37 - Crude, filtered oil from Aktobe..... | 49 |
| Figure 38 - Berea sandstone core samples and powder | 50 |
| Figure 39 - General structure of investigated polymers (Quadri, 2015)..... | 50 |
| Figure 40 - Polymer samples | 51 |
| Figure 41 - Anton Paar MCR 301 Rheometer | 53 |
| Figure 42 - Cone plate Measuring System for the MCR | 53 |
| Figure 43 - Cylindrical Measuring System for the MCR | 53 |
| Figure 44 - Hamilton Beach Single Spindle Drink Mixer HMD 200..... | 54 |
| Figure 45 - Core saturator | 54 |
| Figure 46 - Core-flooding apparatus..... | 55 |
| Figure 47 - Oil displacement test sequence | 56 |
| Figure 48 - The effect of concentration and shear rate on rheological behavior and viscosity of Sav 10..... | 59 |
| Figure 49 - The effect of concentration and shear rate on rheological behavior and viscosity of Sav 19..... | 59 |
| Figure 50 - The effect of concentration and shear rate on rheological behavior and viscosity of Sav 10 XV..... | 60 |
| Figure 51 - Rheological comparison of polymers with increase in shear rate at the same polymer concentration..... | 60 |
| Figure 52 - The effect of temperature on rheological properties of 2500 ppm Sav 10..... | 61 |
| Figure 53 - The effect of temperature on rheological properties of 2500 ppm Sav 19..... | 61 |
| Figure 54 - The effect of temperature on rheological properties of 2500 ppm Sav 10 XV | 61 |
| Figure 55 - The effect of temperature on rheological properties of 1500 ppm Sav 10..... | 62 |

| | |
|--|----|
| Figure 56 - The effect of temperature on rheological properties of 1500 ppm Sav 19..... | 62 |
| Figure 57 - The effect of temperature on rheological properties of 1500 ppm Sav 10 XV | 62 |
| Figure 58 - The effect of temperature on rheological properties of 3000 ppm Sav 10..... | 62 |
| Figure 59 - The effect of temperature on rheological properties of 3000 ppm Sav 19..... | 62 |
| Figure 60 - The effect of temperature on rheological properties of 3000 ppm Sav 10 XV | 63 |
| Figure 61 - Thermal degradation of the polymers | 63 |
| Figure 62 : a - Mechanical degradation of 2500 ppm polymer solutions during different time interval; b -Mechanical degradation of 1500 ppm polymer solutions during different time interval; c - Mechanical degradation factor of 2500 ppm polymer solutions during different time interval.; d - Mechanical degradation factor of 2500 ppm polymer solutions during different time interval. | 65 |
| Figure 63 - Polymers' viscosity loss during 60 days at 80 °C..... | 66 |
| Figure 64 - Viscosity degradation degree during 60 days at 80 °C..... | 66 |
| Figure 65 - Resistance factor as a function of injection rate for 9 polymer solutions. | 67 |
| Figure 66 - Viscosity degradation factor of all polymer solutions as a function of injection rate. | 68 |
| Figure 67 - Differential pressure of polymer flooding vs injected pore volume | 69 |
| Figure 68 - Oil recovery of brine and polymer flooding and differential pressure as functions of injected pore volumes | 71 |
| Figure 69 - Resistance and degradation factor as a function of injection rate | 71 |

List of Tables

| | |
|---|----|
| Table 1 - Petro-physical properties of the Uzen field's oil productive layers | 16 |
| Table 2 - The Uzen field oil composition | 17 |
| Table 3 - Injection and formation water properties of different productive horizons. | 18 |
| Table 4 - Distribution of initial and produced oil reserves by technological sub-objects up to 2011 year..... | 18 |
| Table 5 - Change of the main development indicators of XIII-XVIII horizons for 2009-07.2014 years | 20 |
| Table 6 - Combination of statistical results of polymer flooding from field and pilot data sets (Zhang et al. 2016)..... | 22 |
| Table 7 - Oil sample properties at certain temperatures | 33 |
| Table 8 - Characteristics of brine..... | 33 |
| Table 9 -The combined percentages of the two used polymers..... | 37 |
| Table 10 - Composition of polymers | 39 |
| Table 11 - Outcomes of the coreflooding | 46 |
| Table 12 - Ion composition and mass of salts for Uzen field formation water..... | 48 |
| Table 13 - Reference oil viscosity | 49 |
| Table 14 - Initial viscosities of polymer solutions..... | 56 |
| Table 15 - Viscosities of polymers solution at different concentrations, temperature of 60 °C, and shear rate of 10.8 s ⁻¹ | 59 |
| Table 16 - Viscosity values and degree of degradation of polymers..... | 64 |
| Table 17 - Physical properties of the sandstone core samples..... | 67 |
| Table 18 - Comparison of initial and effluents viscosity values with degradation factor. | 68 |
| Table 19 - Petro-physical properties of the core..... | 70 |
| Table 20 - Major outcomes of the oil displacement experiment | 70 |

Abbreviations

AM Acrylamide

ATBS Acrylamid-Tert-Butyl-Sulfonate

CEOR Chemical Enhanced Oil Recovery

DR Degradation factor

EOR Enhanced Oil Recovery

HPAM Partially hydrolyzed polyacrylamide

MCR Modular Compact Rheometer

NVP n-Vinyl-Pyrolidone

OOIP Original Oil in Place

RRF Residual Recovery factor

RF Recovery factor

Symbols

Latin

K Permeability

P Pressure

S Saturation

T Temperature

Greek

μ Viscosity

1. Introduction

1.1. Background

Polymer flooding is one of the most applied CEOR methods and tertiary oil recovery techniques in general (Sheng, 2014). The main mechanism of polymer flooding is reduction of mobility of injected fluid. Addition of polymer solution to displacing fluid (water) leads to an increase in its viscosity. (Salmo et al., 2017). Thus, this technique increases the oil recovery by improving sweep efficiency due to reduced mobility ratio (Neil et al. 2012). Moreover, polymer flooding technique has an economic impact since amount of water used in the system is decreased (Sheng, 2011). Based on analysis made by Sheng (2014), since most reservoirs already undergo secondary recovery techniques, polymer flooding might be applied at further stages as of oilfield life, as a tertiary recovery technique to increase oil recovery. Polymer flooding has a higher success rate compared to other chemical EOR techniques (Sheng, 2014). Field implementations data of polymer flooding, which is presented in several studies, confirms effectiveness of polymer flooding over conventional water flooding. Yang with colleagues (2006) reported results of two pilot tests of polymer flooding in China (Daqing field). Injection of high-molecular weight, high concentration polymer solution into field led to an increase of cumulative oil recovery after the water flooding. The result of the first test indicates a 19.8–22.9% rise in incremental oil recovery, while second tests presented approximately 19 % increase. Before pilots, authors conducted core flooding experiments, which resulted in a 20% growth of OOIP over water flooding.

According to Sheng (2011), two most frequently applied types of polymers are synthetic polymers and biopolymers. The most popular synthetic polymer is partially hydrolyzed polyacrylamide (HPAM) and its derivatives. A typical biopolymer is xanthan gum. However, implementation of xanthan gum in polymer flooding is impeded by poor infectivity and biodegradation. HPAM solutions are not stable in conditions with elevated temperatures and salinity level reservoirs, which causes a loss of polymers viscosity (Sheng, 2011). It is worth mentioning that conventional polymer flooding is highly restricted by several conditions (Sheng, 2011). Namely, efficiency of polymer flooding drops dramatically in reservoirs with high temperature and salinity (Yanbiao and Jiangbo, 2005). Salinity of formation and composition of brine are critical parameters of successful

polymer flooding implementation. Generally, application of polymer flooding in high salinity (more than 85000 ppm) reservoirs has impact on oil recovery similar to water flooding (Algharaib, 2014). In addition to that, polymer flooding performance is substantially affected by reservoir temperature. Many researchers (Sheng, 2011; Taber et al., 1997; Zhang et al., 2016), who gathered and compared data from literature and field implementation claim that typical values of formation temperature are lower than 93.3 °C. However, addition of specific functional group to the structure of polyacrylamide to form copolymers allows us to increase stability of polymer for different conditions (Sheng, 2011). For instance, Chinese copolymer KYPAM, which is formed by incorporating of functional radical to acrylamide showed significant salinity tolerance in comparison with hydrolyzed polyacrylamide (Sheng, 2011). Additionally, rock type plays serious role in successful application of polymer flooding. The majority of polymer flooding field implementation were designed for application in sandstone reservoirs (Sheng, 2011). Carbonate reservoirs are less preferable due to high adsorption of anionic polymers such as HPAM to rock surface and low formation permeability. Therefore, screening of certain polymer for implementation on specific field have to be done considering complexity of parameters. These are formation water salinity and composition, reservoir temperature, formation permeability and porosity (affect injection rate), rock type, oil viscosity (Sheng, 2011; Zhang et al., 2016).

Based on variation of listed field's parameters, polymer stability under certain reservoir conditions has to be investigated. Stability is presented by resistance to mechanical, thermal, chemical, and biological degradation (Sheng et al., 2015). Chemical degradation is primarily influenced by concentration of salt ions and oxygen, which are present in formation water. For instance, HPAM reacts with divalent and multivalent ions of brine resulting loss in viscosity of polymer solution. Mechanical degradation is caused by increased shear rate near wellbore area due to injection of polymer solution into formation. It creates breakage of polymer molecules and reduction of viscosifying ability of displacing solution. Thermal degradation results in viscosity loss of polymer due to exposure of solutions to elevated temperatures. This is especially valid for polyacrylamide-based polymers, which exhibit dramatic viscosity loss at elevated temperatures due to increased rate of hydrolysis (Sheng, 2011). Biodegradation is more typical for biopolymers, however, synthetic polymers could be also biodegradable due presence of certain bacteria. For example, sulfate-reducing bacteria are able to decompose molecules of HPAM (Luo et al., 2006).

According to Mullayev et al. (2017), Uzen field formation water salinity level varies from 58000 to 77000 ppm and temperature range is equal to 58 – 63 °C. Even if these values cannot be considered high, traditional EOR grade polymer will be less effective in such conditions (Sheng, 2011). However, there are number of salinity and temperature tolerant polymers, which can perform well in this environment. The addition of special-designed monomer to the polymer structure results in resistance to thermal and chemical degradation (Sheng, 2011). For example, n-Vinyl-Pyrrolidone (NVP) monomer provides co and ter-polymers with salinity tolerance (Wang, 2012) and acrylamide-tertiary-butyl sulfonic acid (ATBS) gives a resistance to thermal degradation (Sandengen, 2018). Thus, such polymers can be a possible candidate for application in the Uzen field.

1.2. Problem definition

Over the past decades, oil has been one of the main sources of energy for mankind. The energy demand around the world continues to grow, while alternative sources of energy have not yet made a significant contribution to global demand (Sheng, 2011). In addition, the rate of discovery of new fields has been steadily declining recently (Sheng, 2011). Thus, improving oil recovery from established fields through primary and secondary recovery methods is crucial to meet the growing global demand for energy. The Uzen field, which is in the west of Kazakhstan, is one of the largest oil deposits in the country. The field was discovered in 1961 and oil production has declined significantly since then, despite a substantial geological reserve of oil. Hence, increasing oil cumulative production of the field will positively affect energy supply in the whole country.

One method to improve oil recovery of mature fields is the application the polymer flooding as tertiary recovery technique. This method was chosen due to specific conditions in the Uzen field such as high water cut and lithological heterogeneity, which causes viscous fingering.

There are number of studies, which showed the efficiency of chemical flooding in the lab and field scale (Yang et al. 2006; Sheng, 2011; Sorbie, 2013; Standnes and Skjevrak, 2016; Zhang et al. 2016). However, a successful application of polymer flooding in the specific field requires a well-designed evaluation and selection process, based on the analysis of field data. In this work, polymer

screening process and core scale flooding in the simulated conditions of the Uzen were conducted to evaluate the most appropriate candidate for the field application.

1.3. Thesis objectives

The main objective of this thesis work is to design and conduct a proper set of laboratory experiments to select an appropriate polymer candidate for the application of polymer flooding in the Uzen field.

1.4 Significance of work

This thesis work was designed to evaluate performance of three synthetic polymers under reservoir conditions of the Uzen field. Consequently, outcomes of this work can be used in future pilot tests or for a further investigation of other potentially applicable polymers as a comparative data. This work can be also developed by the combination of the chosen polymer candidate with other chemicals such as surfactants and alkali (ASP flooding). Finally, the results of this investigation can be a good improvement in knowledge of polymer stability in conditions of Kazakhstani field.

2. Literature review

2.1. The Uzen field characteristics

This subsection includes information about Uzen field, which was found in open sources and compiled in a book on the Uzen deposit, authored by Mullayev et al. (2017).

Uzen field was discovered in 1961 and located in western region of Kazakhstan near pre-Caspian Basin. The oil reserves were estimated at 8.6 billion barrels with a total recovery factor of 44 % (Sparke et al., 2005). This is a highly faulted sandstone formation with high lithological heterogeneity, which consists of multi-layered productive horizons with the average thickness of 40-55 m and depth of 852 to 1700 m. Figure 1 shows structure of the formation with oil in gas distribution in the deposit. As it can be seen from the illustration, the oil-bearing zones are located in XIII – XVIII horizons. Average petro-physical characterization of oil productive layers of Uzen field is given in Table 1.

Table 1 - Petro-physical properties of the Uzen field's oil productive layers

| Formation | Property | | | | | |
|------------|------------------|--------------------------|--------------------------------|----------------------------------|---------------------------|----------------------------|
| | Average porosity | Average permeability, mD | Average initial oil saturation | Average initial water saturation | Average oil density, g/cc | Average, oil viscosity, cp |
| Uzen field | 0.22-0.24 | 10-1200 | 0.69 | 0.31 | 0.768 | 3.14-4.22 |

The oil of this formation is characterized as light, highly paraffinic (17-20 %), resinous (8-20 %) with a low Sulphur content (0.1-0.24 %). The Uzen field oil composition is given in Table 2.

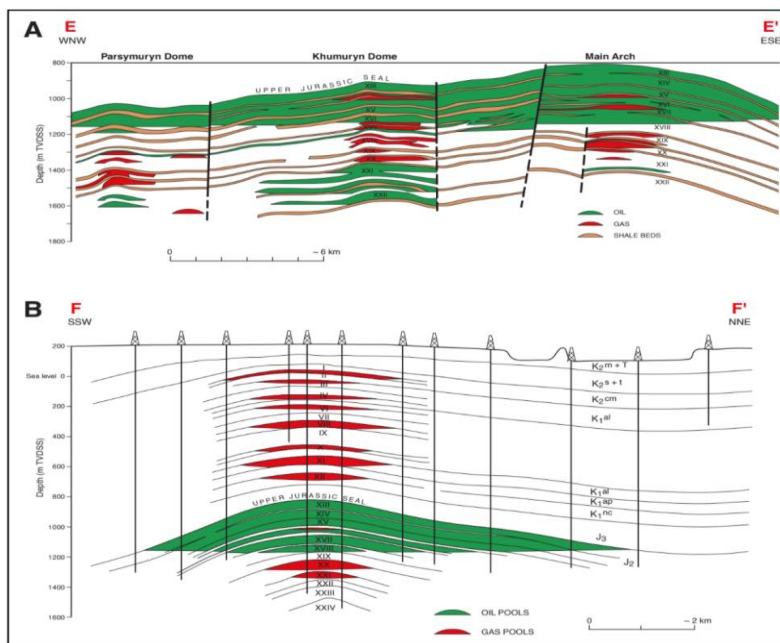


Figure 1 - Structural sections of the Uzen field with hydrocarbon distribution: a) - along the fold axis; b) - perpendicular to the fold axis (Ulmishek, 1990)

Table 2 - The Uzen field oil composition

| Component content, mole fraction % | Productive horizon | | | | | |
|---------------------------------------|--------------------|-------|-------|-------|-------|-------|
| | XIII | XIV | XV | XVI | XVII | XVIII |
| CO ₂ | 0.09 | 0.11 | 0.09 | 0.08 | 0.06 | 0.06 |
| N ₂ | 0.81 | 0.66 | 0.30 | 1.18 | 0.38 | 0.41 |
| C ₁ | 20.99 | 22.85 | 27.13 | 25.35 | 22.42 | 23.98 |
| C ₂ | 8.98 | 8.50 | 8.18 | 6.89 | 8.45 | 9.01 |
| C ₃ | 8.06 | 6.79 | 5.69 | 4.64 | 5.85 | 6.19 |
| i-C ₄ | 1.99 | 1.60 | 1.48 | 1.15 | 1.27 | 1.33 |
| n-C ₄ | 3.77 | 2.88 | 2.79 | 2.18 | 2.56 | 2.64 |
| i-C ₅ | 1.99 | 1.82 | 1.33 | 2.11 | 1.71 | 1.69 |
| n-C ₅ | 2.11 | 2.19 | 1.76 | 2.44 | 1.52 | 1.50 |
| C ₆ | 4.32 | 5.49 | 2.52 | 6.10 | 5.78 | 5.55 |
| C _{7+B} | 4.31 | 5.94 | 2.45 | 6.68 | 8.59 | 8.18 |
| Residue | 42.58 | 41.23 | 46.28 | 41.23 | 41.40 | 39.47 |
| Molecular weight, g/mole | 195 | 190 | 188 | 199 | 193 | 192 |

Table 3 shows ion composition of the injected and formation water. It is important to mention that, the current method of oil recovery is water flooding. According to the table, the concentration of Uzen field's formation water does not exceed 77000 ppm. The prevailing are monovalent particles, which are less crucial to HPAM based polymers (Sheng, 2011). Thus, application of HPAM based co and ter-polymers may be appropriate.

Table 3 - Injection and formation water properties of different productive horizons.

| Water type | Ions, mg/l | | | | | | Mineralization, g/l | pH | Density, g/cm ³ |
|----------------------|------------------|------------------|---------------------------------|-----------------|-------------------------------|--------------------------------|---------------------|-----|----------------------------|
| | Ca ⁺⁺ | Mg ⁺⁺ | Na ⁺ +K ⁺ | Cl ⁻ | SO ₄ ²⁻ | HCO ₃ ³⁻ | | | |
| Inject. water | | | | | | | | | |
| Sea water | 450 | 780 | 3861 | 6390 | 3360 | 250 | 15.09 | 7.0 | 1.009 |
| Volzhskaya | 44 | 14.4 | 190.8 | 255 | 150 | 83 | 0.73 | 7.0 | 1.000 |
| Sewage | 3000 | 900 | - | 31950 | 1200 | 458 | 51.4 | 6.5 | 1.036 |
| Form. water | | | | | | | | | |
| XIII level | 3237 | 1088 | 17599 | 35241 | 715 | 440 | 58 | - | 1.037 |
| XIV level | 3220 | 1140 | 17034 | 34538 | 668 | 420 | 56 | - | 1.037 |
| XV level | 4231 | 1230 | 21763 | 43788 | 950 | 221 | 72 | - | 1.046 |
| XVI level | 4448 | 1300 | 23426 | 46731 | 832 | 350 | 77 | - | 1.049 |
| XVII level | 3199 | 900 | 17663 | 34711 | 770 | 398 | 57 | - | 1.037 |
| XVIII level | 4364 | 1200 | 23567 | 46573 | 1020 | 380 | 77 | - | 1.048 |

Based on the structure and permeability of the reservoirs, all productive horizons of the Uzen field were divided into three technological sub-objects (TS). The TS-1 includes mainly high-permeable (>300 mD) reservoirs. The TS-2 consists of deposits with permeability of 50-300 mD and considered as medium-permeable. The last one is TS-3, which consists of zones of low permeability (< 50 mD). The data on oil reserves in each of these sub-objects is presented in the Table 3. Obviously, the production of high permeable zones was higher than that of reservoirs with lower permeability.

Table 4 - Distribution of initial and produced oil reserves by technological sub-objects up to 2011 year

| Technological sub-objects | Initial geological oil reserves, thousand tons | Produced oil reserves up to 2011, thousand tons | Remaining geological oil reserves, thousand tons | Percentage of residual oil reserves by TS | Ratio of produced to remaining oil reserves, % |
|---------------------------|--|---|--|---|--|
| Total | 986010 | 317297 | 668713 | 100 | 32.17 |
| TS-1 | 164334 | 55293 | 109041 | 16 | 33.64 |
| TS-2 | 506028 | 218675 | 287353 | 43 | 43.21 |
| TS-3 | 315648 | 43329 | 272319 | 41 | 13.72 |

Figure 2 demonstrates the production history of the Uzen field since the very discover up to the 2008, while Figure 3 gives a visual representation of main technological indicators of production from XIII-XVII horizons for 2009 to 07.2014. Unfortunately, more recent data was not available. It is clear that, both oil production rate and cumulative oil production decreased dramatically since the 1970s and began to rise in the late nineties. The growth stopped in the 2009 with a further gradual decrease up to the first half of 2014.

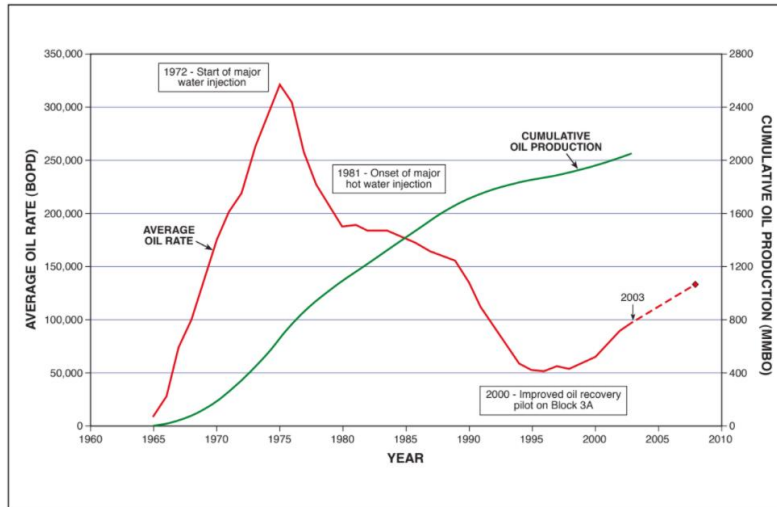


Figure 2 - Production History of the Uzen Filed for 1965-2008 (C & C Reservoirs, 2010)

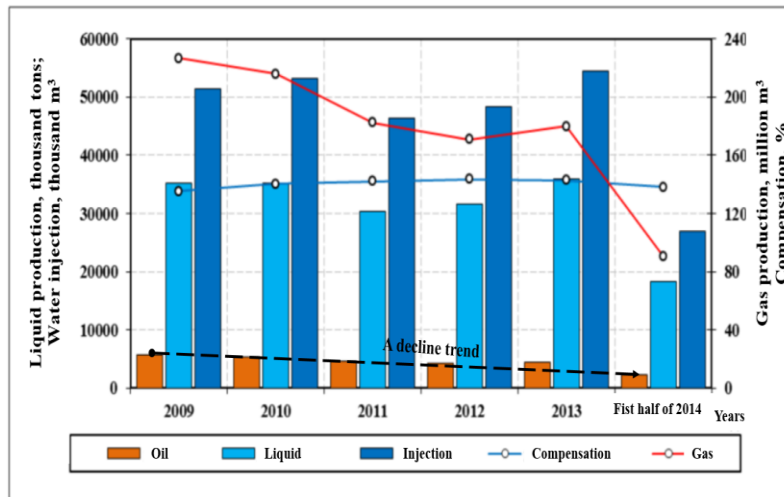


Figure 3 - Dynamics of the main technological production indicators of oil-bearing horizons in the Uzen field for 2009 - 1st half of 2014

Table 5 provides numerical values of indicators, which were graphically represented on the Figure 3. As follows from the data presented, the cumulative liquid production raised by 16.8 %, while annual oil production decreased by 20.4 % for the given period.

Table 5 - Change of the main development indicators of XIII-XVIII horizons for 2009-07.2014 years

| Indicators | Year | | | | | |
|--|----------|----------|----------|----------|----------|------------------------------|
| | 2009 | 2010 | 2011 | 2012 | 2013 | 1 st half of 2014 |
| Oil production, thousand tons | 5685.5 | 5393.1 | 4558.7 | 4297.0 | 4494.4 | 2260.5 |
| Cumulative oil production, thousand tons | 309443.0 | 314837.0 | 319395.7 | 323692.8 | 328187.1 | 330447 |
| Liquid production, thousand tons | 35202.3 | 35239.7 | 30419.5 | 31572.1 | 35883.0 | 18297.0 |
| Cumulative liquid production, thousand tons | 790966.0 | 826205.7 | 856625.3 | 888197.4 | 924080.4 | 942378.0 |
| Average water cut, % wt. | 83.8 | 84.7 | 85.0 | 86.4 | 87.5 | 87.6 |
| Recovery factor | 0.314 | 0.319 | 0.324 | 0.328 | 0.333 | 0.335 |

According to the available information, the only chemical EOR method applied in the Uzen field was the pilot injection of low-concentration Surfactants (0.05% wt) in the XIII and XVIII horizons (low permeable zone). However, this method was applied almost 40 years ago in parallel with other operations such as intensive drilling of new wells, hot water injection / cyclic injection (due to high content of paraffins), and reconstruction of pressure maintenance systems. Hence, it is difficult to assess the effectiveness of the Surfactant flooding application. Despite all this, authors were able to evaluate total additional recovery for the period of low-concentration surfactant application (1981 – 1986 years). The total incremental oil production was 5.42 MMBBL, including 4.52 MMBBL (83.4 %) from the surfactant injection, which can be considered as a very successful application. However, this technique was applied only in the TS-3 zones of low permeability.

The application of surfactant flooding itself in other sections of the field was difficult due to viscous fingering in high permeable zones (TS-1 and TS-2). Another important problem to address is high water cut of the reservoir. According to the Table 5, the average water cut of the field was equal to 87.6 as of the first half of 2014 year and the volume of the total water injected for the whole period of field development 4 times higher than the volume of oil produced.

Combining all the data above, it can be assumed that the application of polymer flooding as a tertiary recovery technique will be effective in the Uzen field due to several reasons. Firstly, high water cut and water consumption during the injection problems can be solved by the polymer

injection, which reduces the amount of the injected and produced water resulting in a positive economic impact (Sheng, 2011). Secondly, polymer flooding reduces viscous fingering in the high permeable zones by the decrease in mobility ratio of the displaced fluid (Sheng, 2011). Finally, the secondary recovery is not more effective as the production decreases every year in current mode of operation (even after the application of thermal EOR). Therefore, the implementation of polymer as tertiary recovery might be applied at the next stage of the field development.

2.2. Reservoir screening criteria for the application of polymer flooding

Ion composition and total dissolved solids of formation water as well as formation temperature are the most crucial parameters to consider during polymer selection. Meanwhile, the addition of special designed functional group to the polymer structure increase salinity and temperature tolerance of polymers (Sheng, 2011). The next important factor to evaluate is the adsorption of polymer to the formation rock surface, which depends on the rock type. For instance, anionic polymers such as HPAM, which is the most popular polymer among synthetic ones due to price and availability, cannot be applied in carbonates as effective as in sandstone reservoirs due to increased number of molecules which are adsorbed to the carbonate rock surface (Sheng, 2011).

Zhang et al. (2016) conducted a complex data analysis of pilot and fields tests to determine ranges of screening criteria for implementation of polymer flooding. Combination of statistical data from 55 polymer flooding pilot and field projects is given in Table 6. The overview provides the conditions, which affect polymer flooding project's performance, including reservoir properties, polymer properties and evaluations. Standard statistics used to characterize the range of the minimum and maximum measurements, mean, and median data set values. It is necessary to emphasize that, Zhang with colleagues focused mostly on sandstone reservoirs, which is a target reservoir of this work.

As a result, the combination of the field data from the previous section and the Table 6 shows that polymer flooding can be applied in the Uzen field. The reservoir parameters from the statistical analysis matches well with the field data of the Uzen deposit.

Table 6 - Combination of statistical results of polymer flooding from field and pilot data sets (Zhang et al. 2016)

| Statistics | | | | |
|--|--------|--------|---------|---------|
| Parameters | Mean | Median | Minimum | Maximum |
| Reservoir temperature (°C) | 68.8 | 70.8 | 26.1 | 93.7 |
| Porosity (%) | 20.79 | 20 | 8.3 | 32 |
| Permeability (md) | 607 | 540 | 17 | 2330 |
| Oil viscosity (cP) | 62 | 32.5 | 2.3 | 285.2 |
| Water salinity (ppm) | 16680 | 7445 | 884 | 84130 |
| Divalent cations (ppm) | 2283 | 311 | 4 | 26000 |
| Polymer molecular weight 10 ⁴ | 1635 | 1585 | 600 | 3150 |
| Polymer concentration (ppm) | 1325 | 1350 | 600 | 2000 |
| Polymer viscosity (cP) | 43.82 | 23 | 15 | 91.1 |
| Injection pressure (Mpa) | 13.84 | 12.76 | 10 | 20.5 |
| Injection rate (PV/A) | 0.146 | 0.13 | 0.057 | 0.34 |
| Well spacing (m) | 192 | 188 | 100 | 310 |
| Polymer slug size (PV) | 0.4122 | 0.406 | 0.033 | 0.8 |
| Water cut before polymer flooding (%) | 91.11 | 94 | 65.6 | 98.14 |

2.3. Polymer Stability

Under certain conditions molecular structure of polymer macromolecules might degrade and break. This process is called polymer degradation (Sorbie, 2013). Polymer degradation is categorized into mechanical, chemical, thermal, and biological. Complex analysis of literature data is presented in investigations of Sorbie (2013), Standnes and Skjevrak (2014), and Seright and Skjevrak (2014).

2.4.1. Mechanical stability

According to Sheng (2011), mechanical stability of polymer is the ability of polymer to retain its viscosifying ability under severe mechanical stress. Polymer solutions are non-Newtonian fluids (Carreau 1972). It means that the viscosity of such a solution changes with a change in shear rate. At lower shear rates polymers exhibit a lower Newtonian region with no significant viscosity alteration, while there is a shear-thinning behavior of polymer solutions with more shear rate applied to the solution. A further increase in shear rate leads to the Upper Newtonian region, where the viscosity of polymer solution will not be affected showing typical Newtonian fluid behavior. Figure 4 illustrates this phenomenon.

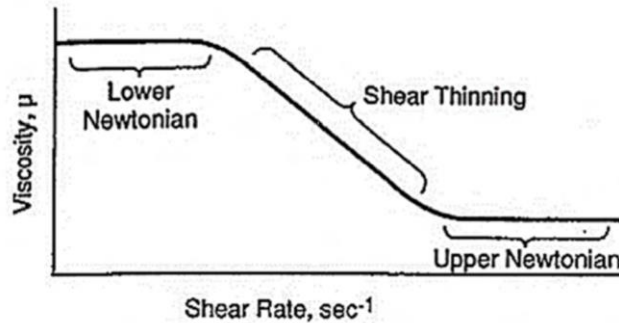


Figure 4 - Viscosity - shear rate relationship of polymer solutions (Green and Willhite 1998)

Standnes and Skjevraak (2014) made an analysis of polymer degradation based on 72 polymer flooding projects including laboratory investigations, pilot, and field tests. HPAM polymer was used in almost all projects that were reviewed by authors. Some of the projects recorded a viscosity loss of polymer solution on at surface conditions due to mechanical degradation. Hence, the manner in which the polymer solution is transported to the wellhead is a crucial factor of polymer stability. Hitts Lake Polymer Injection project, which was conducted by Greaves (1984) reported that removal of chokes in the polymer injection process helped to reduce mechanical damage. It is widely believed that usage of tubes during transportation of the polymer solution has minor effect on the viscosifying ability of the polymer which is supported by the recorded results. It is also known that, at high shear rates when the polymer solution is injected into formation through perforations, polymer degrades and loses its viscosity. Increased number of the perforations shots on certain length is one approach to reduce pressure drop when polymer is injected to reservoir.

Shearing effect on viscosity of polymer solution is shown on Figure 5 and 6. HPAM (**Ошибка! Источник ссылки не найден.**6) and Xanthan gum (**Ошибка! Источник ссылки не найден.**5) polymers were used in this investigation. It is evident from the graph that, all solutions exhibited a strong shear-thinning behavior with HPAM solution demonstrating less sensitive shear dependence than Xanthan gum. Comparison of solutions, which were subjected to shear stress of different level before the measurement (presheared solutions), with unsheared polymer solution are given for both experiments. Presheared solutions were exposed to shearing through consolidated sandstone core at different rates. It is clear that, Xanthan gum polymer solution is exceedingly shear stable after exposure to severe shear rare in both cases. This can be explained

by presence of rigid rod structures in Xanthan gum molecules. Meanwhile, viscosity of HPAM polymer solution appeared to be highly influenced by even moderate level of shearing due to flexible coil molecules (Seright et al., 1983).

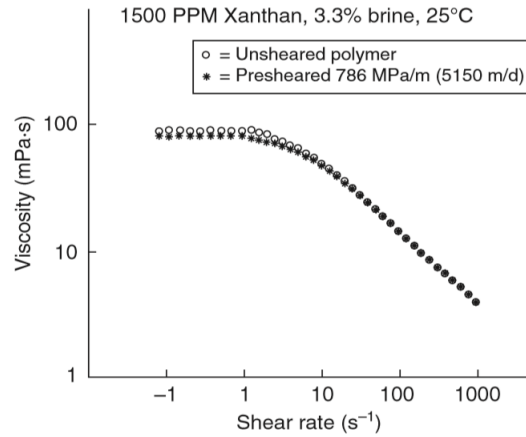


Figure 5 - Viscosity loss of a xanthan solution with increase of shear rate in Berea sandstone core; not significant influence was detected (Seright et al., 1983).

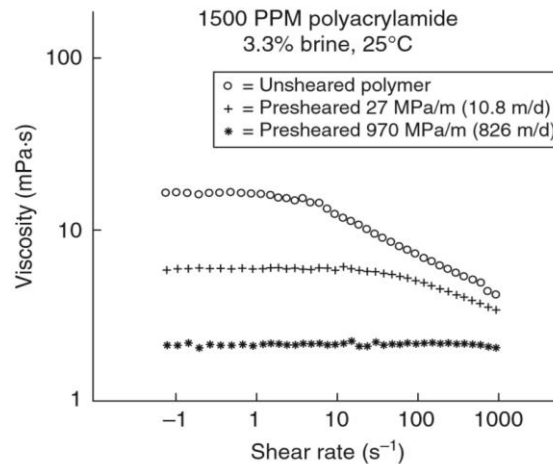


Figure 6 - Viscosity loss of a HPAM samples (unsheared and presheared) with increase of shear rate in Berea sandstone core; not significant influence was detected (Seright et al., 1983).

Higher flow rate and distances with decreased permeability of porous media lead to increased mechanical degradation (Sheng, 2011). There are higher shear stresses acting on the polymer solution when porosity is low. In that case the probability of polymer molecules breakage and severe viscosity loss is higher. In addition, molecular weight of polymer directly affects rate of

mechanical degradation of the injected polymer. More molecular weight of polymer causes higher exposure to mechanical degradation because of increased flow resistance of large molecules. Consequently, these molecules experience more elongation stresses and breakage occurs (Sorbie, 1991; Luo et al., 2006). As a result of this breakage smaller pieces of original polymer molecules appear in the solution.

2.4.2. Chemical stability

Based on research of Yang and Taber (1985), there are many variables, which can affect chemical stability of polymer solution. These are temperature, salinity and hardness, presence of biocides, metal cations, pH scale, chemical additives, and hydrogen sulfide (H₂S). However, authors found out that the rate and degree of polymer solution chemical degradation mainly depend on three major parameters, which are oxygen concentration, salinity, and iron content in the solution. For instance, polyacrylamides could be stable under 93.3 °C for 500 days if concentration of oxygen in the solution is low. Moreover, viscosity of polymer solution may raise during this period. This effect will be also described further.

2.4.2.1. Effect of oxygen on chemical stability of polymers

Figure 7 represents the effect of oxygen content in the system on polymer viscosity in a long period of time at 90 °C. At the low concentration of oxygen viscosity of the polymer solution decreased slightly compared to gradual drop in the presence of significant oxygen concentration. Yang and Taber (1985) made a conclusion that polymer degradation occurs until there is no oxygen left in the system. Luo et al. (2006) confirmed this statement (see Figure 7). In all three cases viscosity drop stopped when oxygen was completely consumed by oxidation reaction.

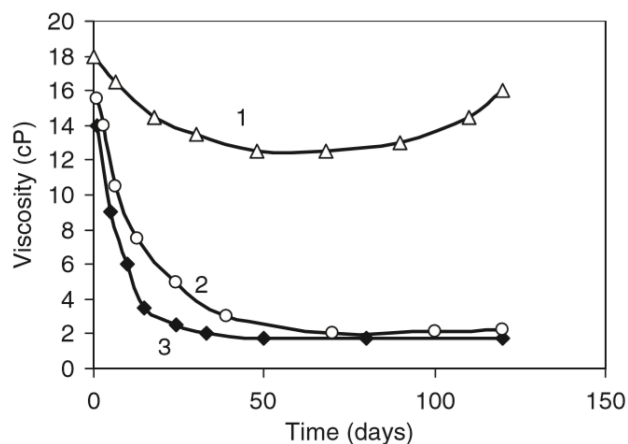


Figure 7 - Influence of oxygen effect on HPAM stability at 90°C combined with three different level of oxygen: 1, low level of oxygen; 2, air; 3, oxygen. Source (Luo et al., 2006).

It can be seen that there was eventual growth of polymer viscosity under conditions of low oxygen concentration. This effect could be explained by raised temperature, which leads to increased hydrolysis of polyacrylamides (Sorbie, 2013). Increased hydrolysis reduced amount of polymer solution, which is adsorbed by surface of media leading to elevated viscosity of the solution. However, it also decreases chemical stability of polymers (Sheng, 2011).

2.4.2.2. Effect of salinity on chemical stability of polymers (Luo et al., 2006)

Figure 8 show the dependence of viscosity on the NaCl and CaCl₂ salts concentration. Clearly, a dramatic viscosity drop was observed with an increase in the concentration of salts in both cases irrespective of the degree of hydrolysis. Moreover, divalent ions of CaCl₂ had a greater impact on the chemical degradation of traditional HPAM polymer solution. The salinity effect of divalent effects causes coagulation and compression of polymer molecules leading to more sever viscosity loss, while monovalent ions have only compressive effect (Sheng, 2011).

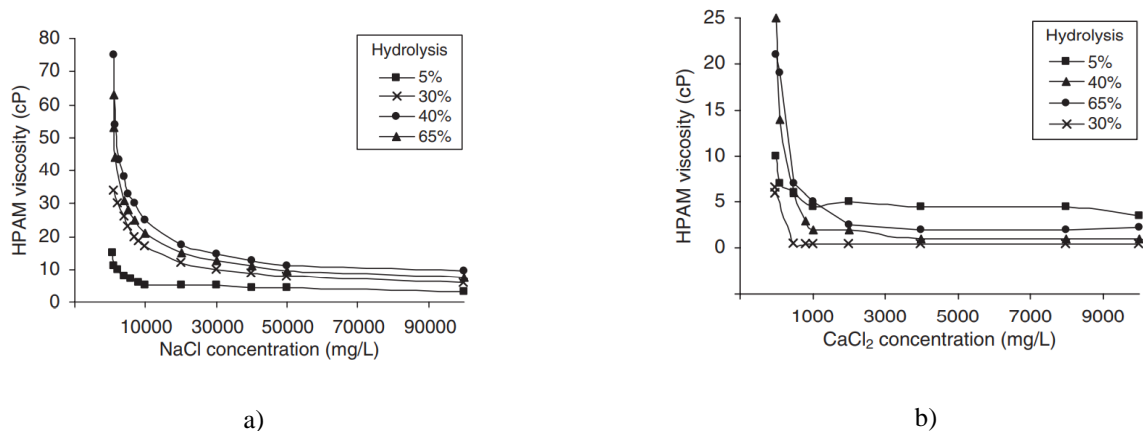


Figure 8: a - Effect of Effect of NaCl concentration on viscosity of HPAM polymer; b - Effect of CaCl₂ concentration on viscosity of HPAM polymer

2.4.2.3. Effect of Iron content on chemical stability of polymer

Polymer solution does not degrade in the presence of certain concentration of iron (II) in the solution if there are no oxygen dissolved or any oxidizing agents (Yang and Treiber, 1985; Seright et al., 2010). Seright and Skjevrak (2014) conducted a series of laboratory experiments and reviewed on effect of different concentration of iron (II) with both oxygen and oxygen-free solutions (See Figure 9 and 10). It is evident that, viscosity loss of polymer solution for any concentration of iron (II) is not significant until concentration of oxygen reached approximately 700 ppb. Another important parameter in this experiment is temperature. It is clear that the viscosity loss and the effect of oxygen and iron (II) are more severe at higher temperature (90 °C). There is even viscosity growth reported at no iron (II) and high oxygen content at 23 °C (see 10). Another factor, which was considered in this investigation is variation of salinity (see **Ошибка! Источник ссылки не найден.**11). After one-week viscosity of the polymer solution at temperature of 90°C and concentration of salt ions accounting for 2.85% of total dissolved solids (TDS) was higher than that of polymer at 23 °C and the same salinity. It is assumed that hydrolysis rate was increased due to high temperature, and this led to raise of viscosity of the solution. Moreover, mild degradation of polymer occurred at this particular conditions. Generally, all other cases were independent of variation of iron (II) concentration. Therefore, polymer degradation by the presence of Iron (II) should be considered with complex analysis of other factors such as high temperature and presence of oxidizing agents.

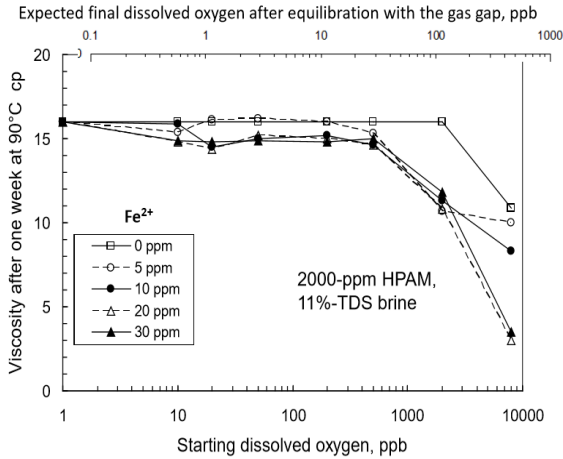


Figure 9 - HPAM viscosity alteration by presence of dissolved oxygen and Fe²⁺ at 90°C (Seright and Skjevrak, 2014).

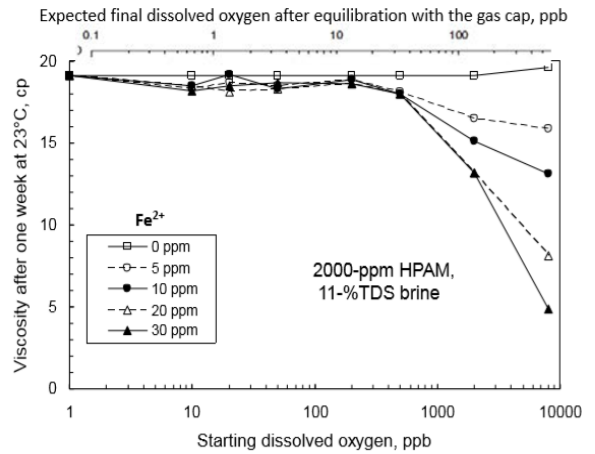


Figure 10 - HPAM-ATBS viscosity alteration by presence of dissolved oxygen and Fe²⁺ at 90°C (Seright and Skjevrak, 2014).

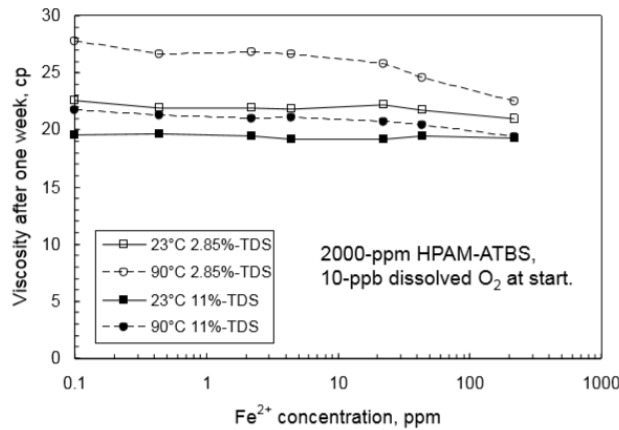


Figure 11 - Effect of Fe²⁺, temperature, and salinity on HPAM-ATBS stability (Seright and Skjevrak, 2014).

2.4.2.4. Ways to reduce chemical degradation used in pilot and field tests

According to the analysis of 72 polymer flooding projects, polymer solutions mainly suffered from high oxygen, salts and iron (II) content in reservoirs (Standnes and Skjevrak, 2014). In overwhelming majority of cases, oxygen scavengers were mixed with mother solution for the purpose of oxygen control. Contact of wetted steel surfaces with the polymer solutions kept at minimum level to avoid increasing of iron (II) concentration in the formation. Another solution to remove iron (II) from the solution is by reacting it with oxygenated water before starting polymer

flooding (Levitt et al., 2011a). This leads to iron (II) precipitation. Consequently, solid particles have to be removed from the solution by filtration. This method was used in pilot test in Canada (Irvine et al., 2012). However, this technique requires significant preparatory measures such as filtration and oxygenation of water, isolation of steel facilities by addition of inert gas and finally, removal of precipitate. Alternative method of minimizing iron (II) in the solution is to add alkaline. Mixing alkaline with polymer solution (HPAM was used in this work) provides it with tolerance to presence of iron (II) and makes it stable (Levitt et al., 2011b).

2.4.3. Thermal stability

Thermal stability of polymers defines as ability of polymers to retain its viscosity under the increase in temperature. The increase in temperature leads to viscosity drop of polyacrylamide polymer solution (Yang and Treiber, 1985; Tan, 1998; Sheng, 2011; Standnes and Skjevraak, 2014; Wu, 2016). This effect is illustrated on the Figure 12. This is due to enhancing of polymer molecules and reduction of the friction between molecules, which cause the viscosity loss. However, for the HPAM polymers, the increase in temperature accelerates the hydrolysis rate of the solution. Subsequently, the viscosity increases slightly, however, higher rate of the hydrolysis will also reduce the chemical stability (Sheng, 2011). Figure 11 from previous sub-section displays this effect. The viscosity of the same solution at the same temperature but with different salinity level had a dramatic difference of viscosities.

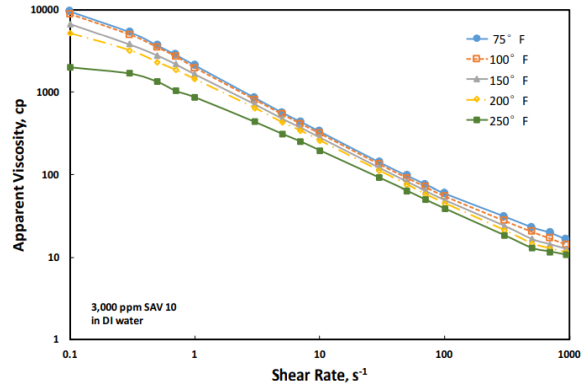


Figure 12 - Effect of temperature on apparent viscosity of HPAM-based polymer with ATBS monomer in the functional structure (Wu, 2016)

Tan (1998) discovered that the gradual increase in the temperature resulted in lower gradient of viscosity degradation compared to the effect of constant temperature as shown on Figure 13. The HPAM polymer used in this paper has been degraded until there was no oxygen left in the system.

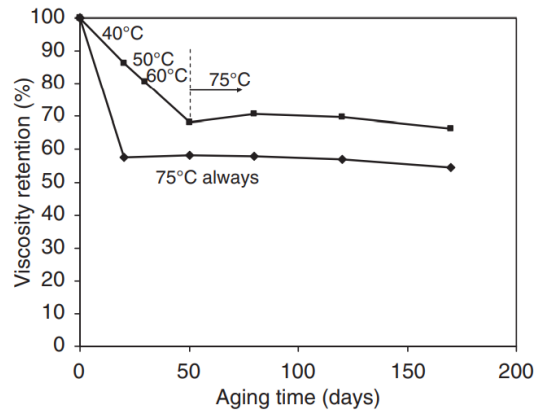


Figure 13 - Difference between gradual temperature increase and the effect of constant temperature (Tan, 1998)

Generally, the elevated temperatures negatively affect the viscosity of the synthetic polymer solutions, which is evident from several papers.

2.4.4. Biological degradation

As reported by Sorbie (2013), biological degradation corresponds to microbial decomposition of polymer macromolecules by bacteria. It can affect the solution in the storage tanks or in pipe-lines before injection or even in low temperature regions of reservoirs. Naturally produced polymers or biopolymers are more susceptible to microorganisms compared to synthetic ones (Rellegadla et al., 2017). This would lead to substantial decrease of biopolymers viscosity (Sheng 2011). Nevertheless, synthetic polymers such as HPAM are also affected by microbial activity (Luo et al., 2006). Sulfate reducing bacteria consumes macromolecules of polyacrylamides as nutrition. A laboratory investigation was conducted on microbial decomposition of polymer solution (Niu et al., 2006). The conditions were: concentration of bacteria in each case was 2% or 10^5 bacteria per 1 milliliter, concentration of polymer was 1000 milligram per liter, room temperature. **Ошибка! Источник ссылки не найден.**14 represents biological degradation of polymer during long period of time by four main type of bacteria in reservoir. SRB stands for sulfate reducing bacteria, HOB – hydrogen oxidizing bacteria, TGB-A and B - total general bacteria A and B. In all cases, microbial decomposition occurred.

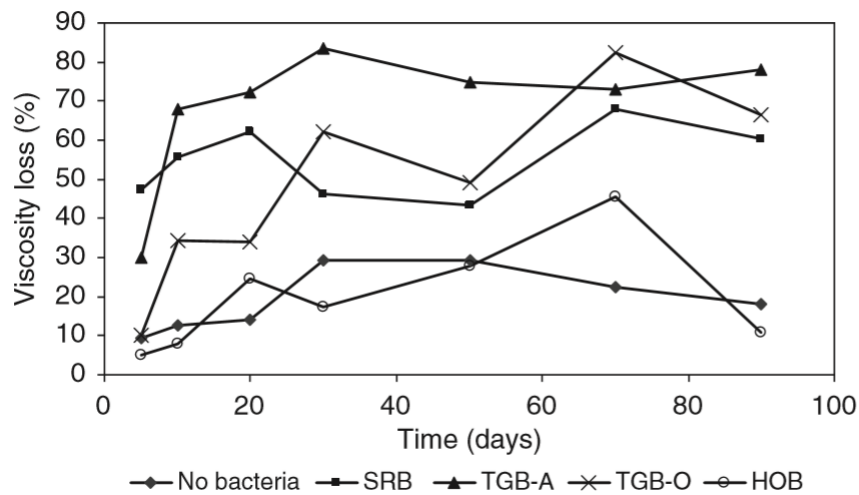


Figure 14 - Bacterial degradation of polymer solution (Niu et al., 2006).

According to the analysis of 72 polymer flooding projects conducted by Standnes and Skjevraak (2014), three projects recorded biodegradation of polymer solutions, which led to loss of polymer viscosity. Two out of three reported bacteria originated from make-up water. The rest one concluded that bacteria appeared from mineral oil during delivery of the solution as an emulsion. In all three cases biocides were added to mother solution to stop further microbial decomposition of the polymer solutions. Effectiveness of biocide was also confirmed in investigations of number of researchers (Sheng, 2011; Sorbie, 2013; Rellegadla et al., 2017; Luo et al., 2006; Chang, 1978; O'Leary et al., 1985). However, certain biocides could influence on performance of polymer in oil recovery process (Sorbie, 2013). Sheng (2011) emphasized toxicity of formaldehyde, which is one of the most popular biocides and was used in variety of implementations. Chang (1978) in his work reported effectiveness of formaldehyde application as biocide in both field and laboratory projects. Small concentration of formaldehyde (25 to 100 ppm) was used in these projects. Therefore, compatibility test must be conducted before application of biocide for control of biodegradation.

2.5. Analogy evaluation

This section includes the review of several works, which were dedicated to the investigation of polymers performance in the variety of experimental conditions, which are similar to that of the Uzen field or have even more hostile environment. All the investigated polymers were modified polymers that are effective to use in reservoirs with medium to high level of salinity and temperature.

2.5.1. Zetag 8187G (Firozjahi et al., 2019)

In this work authors studied performance of two synthetic polymer solutions at almost the same temperature as in Uzen field reservoir, while salinity level is 2 times higher. The first one is SAV 37, ter-polymer containing n-VP functional group, and designed to work efficiently in the harsh conditions. In this work SAV 37 is taken as comparison polymer. The main object of this investigation is application of Zetag 8187G, which is co-polymer of acrylamide and quaternized cationic monomer. Rheological behavior of polymers under variation of temperature and salinity level is studied in the lab scale with a follow up investigation of oil recovery efficiency by the polymer flooding.

Table 7 and 8 provides the information about oil properties and water composition, which were used in this study. Brine was prepared by addition of 10000 ppm NaCl to water.

Table 7 - Oil sample properties at certain temperatures

| Temperature, (°C) | Density (g/cm ³) | Viscosity (cp) |
|-------------------|------------------------------|----------------|
| 25 | 0.8421 | 34.847 |
| 65 | 0.8515 | 5.0247 |

Table 8 - Characteristics of brine

| Electrolyte | Weight (g) | Mw (g/mol) |
|-------------------|------------|------------|
| NaCl | 110 | 58.44 |
| KCl | 2 | 74.56 |
| CaCl ₂ | 5 | 110.98 |
| MgCl ₂ | 33 | 95.22 |

Polymer properties: Zetag 8187G with molecular weight of 9-16 MM and density of 2-5 g/cc. And comparative polymer sample, SAV 37, with molecular weight of 0.7 MM and density of 0.6-0.9 g/cc.

Two cores (AS-1, AS-2) were made up from sandstone blocks of Aghajari formation of Ahwaz Iran. The first and the second core had an approximately the same permeability and porosity

accounting for 18 mD and 19.5 % respectively. Interestingly, the sandstone core samples, which were used in this paper have almost the same characteristics as that of TS-3 object in the Uzen field.

Authors conducted first water then polymer flooding on two prepared cores. In addition, a post flush water flooding after the polymer injection was carried out in AS-2 core to record residual resistant factor (RRF) for the evaluation of permeability reduction caused by the polymer flooding. Resistance factor (RF) was measured as well. According to Wang et al. (2018), RF and RRF are the crucial criteria for determination of polymer flooding's effectiveness in oil displacement. RF is a mobility ratio of fluids, referring to a difference in between resistance to flow by water and polymer solutions in porous media. RRF is the difference in permeability between brine flooding through core before and after polymer injection. RRF is great measure of permeability reduction caused by polymer retention. Conditions of core flooding experiments are temperature of 65 °C, which is almost equal to that of the Uzen, formation water salinity level of 150000 ppm, and 2000 psi of the confining pressure.

Figure 15 and **Ошибка! Источник ссылки не найден.**6 demonstrate the influence of salinity and temperature variation on viscosity of fluids, respectively. As a result, both temperature and salinity tolerance of Zetag 8187G was higher than that of SAV 37. The long-term thermal stability experiment showed Zetag 8187G can be stable under the harsh conditions for six months. (see Figure 17).

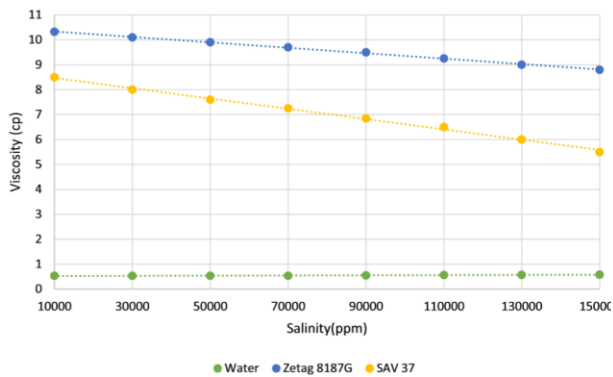


Figure 15 - Polymer viscosity alteration due to different level of salinity in high temperature condition

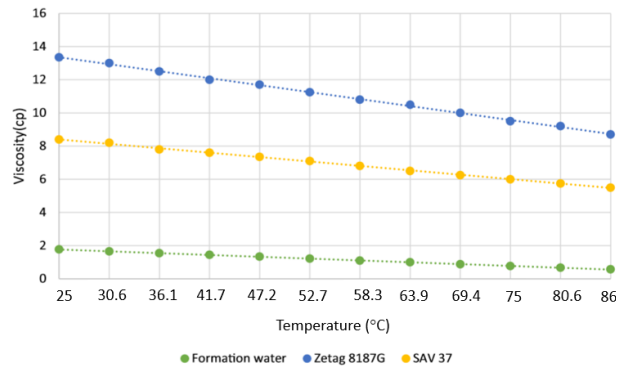


Figure 16 - Polymer viscosity alteration due to different level variation of temperature in 150,000 ppm salinity

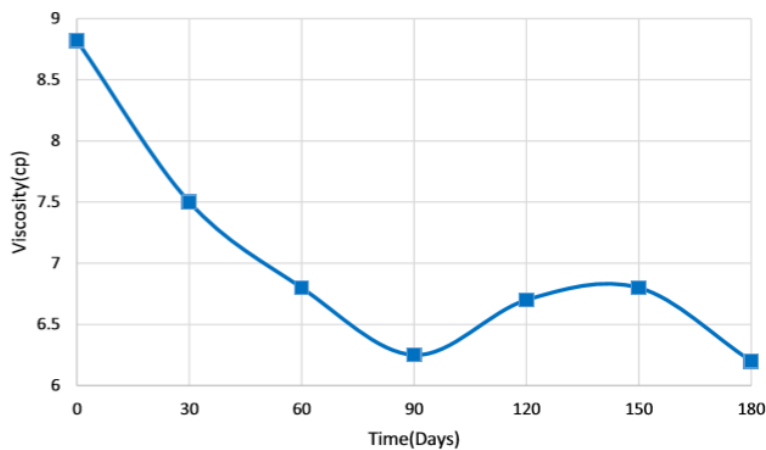


Figure 17 – Long-term polymer stability of Zetag 8187G (2000 ppm of polymer solution, temperature of 86 °C, and salinity level of 150,000 ppm,)

Ошибка! Источник ссылки не найден.18 and Ошибка! Источник ссылки не найден.19 show the results of core flooding experiments. The injection of polymer solution provided better performance in both increasing oil recovery factor (increased in 2 times) and decreasing oil saturation in comparison with water flooding. As RF values, it constituted 5.01, which is appropriate value for high molecular weight of polymer. The measurement of RRF showed 5 mD reduction of core effective permeability, which is acceptable. Thus

Therefore, the injection Zetag 8187G demonstrated good efficiency of core scale oil displacement at the temperature, which was closed to that of Uzen field and salinity of 150000 ppm. This study demonstrated that application of polymer in such conditions provides much better results than the secondary recovery by water.

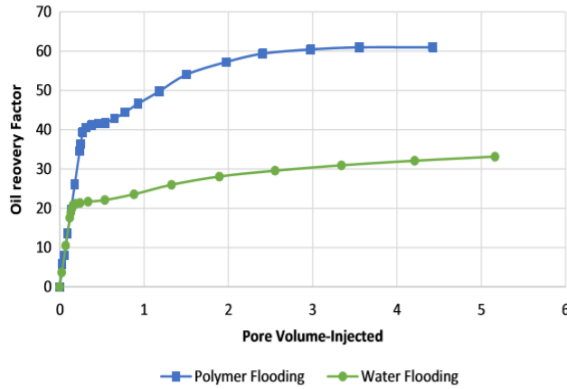


Figure 18 - Pore Volume Injected vs. Oil recovery factor for water and polymer flooding

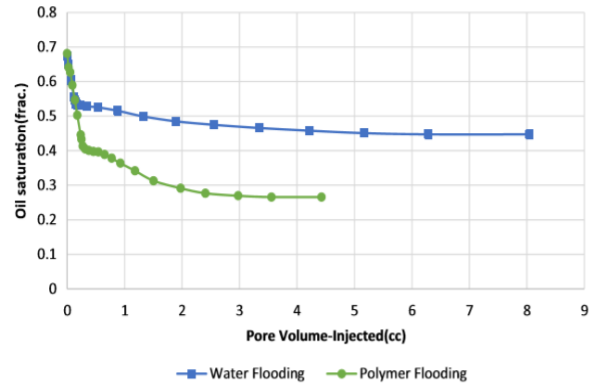


Figure 19 - Residual oil saturation vs. Pore Volume Injected for water and polymer flooding

2.5.2. Combination of SAV37 and AN125VHM (Firozjahi et al., 2019)

In this work authors studied performance of polymer solution containing two synthetic polymers SAV37 and AN125VHM. SAV 37 is described in previous work and AN125VHM is polymer, one quarter of which is ATBS functional monomer. The variation of temperature, salinity and polymers concentration was applied to investigate rheological behavior of these synthetic polymers. In addition, the oil displacement test was set up to evaluate the efficiency of such approach.

Two cores (AS-1, AS-2) were made up from the sandstone blocks of Aghajari formation of Ahwaz, Iran. The first core had a porosity of 19.5 % and permeability of 18 mD. The second one had a porosity of 12.1 % and permeability of 17.5 mD. These cores have the similar parameters as the sandstone rock in the low permeable zone in the Uzen field (TS-3 block).

Additionally, the same oil and formation water samples were used as in the previous work (see Table 7 and 8).

Researchers prepared 5 solutions with different weight proportion of SAV 37 and AN125VHM to obtain 6000 ppm total concentration of polymers. Table 9 provides information about total composition of final solutions.

Table 9 -The combined percentages of the two used polymers

| Solution | SAV37 | AN125VHM |
|-----------------|--------------|-----------------|
| 1 | 2 gr (100%) | 0 |
| 2 | 1.4 gr (70%) | 0.6 gr (30%) |
| 3 | 1 gr (50%) | 1 gr (50%) |
| 4 | 0.6 gr (30%) | 1.4 gr (70%) |
| 5 | 0 | 2 gr (100%) |

Firstly, the thermal stability of prepared polymer solutions with different compositions was investigated as shown on **Ошибка! Источник ссылки не найден.**²⁰. The most viscous polymer solution among the others was solution of 100% of AN125VHM. This is due to the high content of ATBS in the chemical structure of AN125VHM. However, this polymer solution had the worst salinity tolerance as shown on the Figure 21.

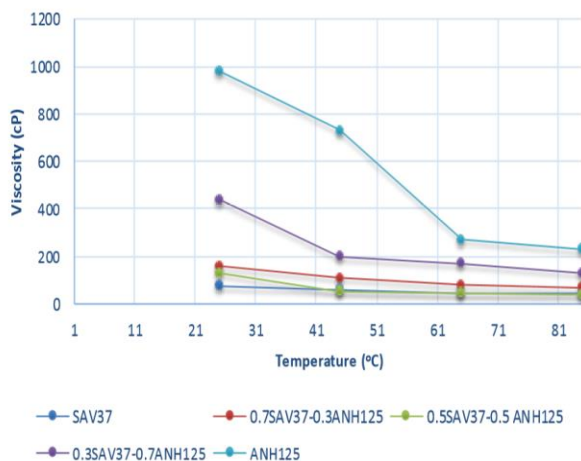


Figure 20 - Effect of increasing temperature on viscosity of 6000 ppm of polymer solution with different weight percentages of two SAV37 and AN125VHM polymer (Salinity of 10000 ppm).

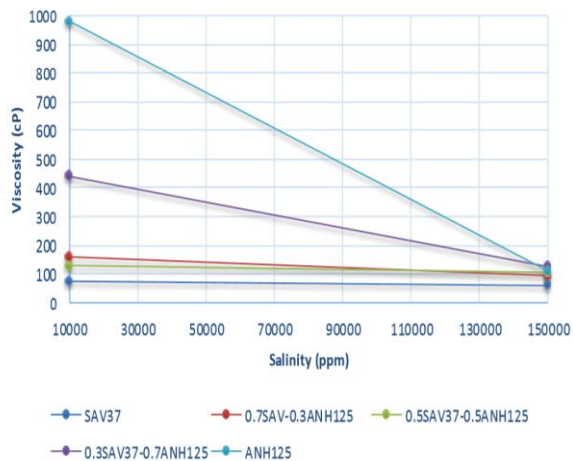


Figure 21 - Effect of increasing salinity on viscosity of 6000 ppm of polymer solution with different weight percentages of two SAV37 and AN125VHM polymer (Room temperature).

Ошибка! Источник ссылки не найден. 22 represents viscosity loss of polymer solutions due to increasing of temperature in constant salinity of 150000 ppm. The most stable solution in these conditions was solution, which contained half of SAV 37 and half of AN125VHM. This is because these polymers contain salinity and temperature tolerant functional monomers equally. Long-term thermal stability test of this solution in which 2000 ppm of polymer solution was stored for month at temperature of 85 °C showed insignificant viscosity loss.

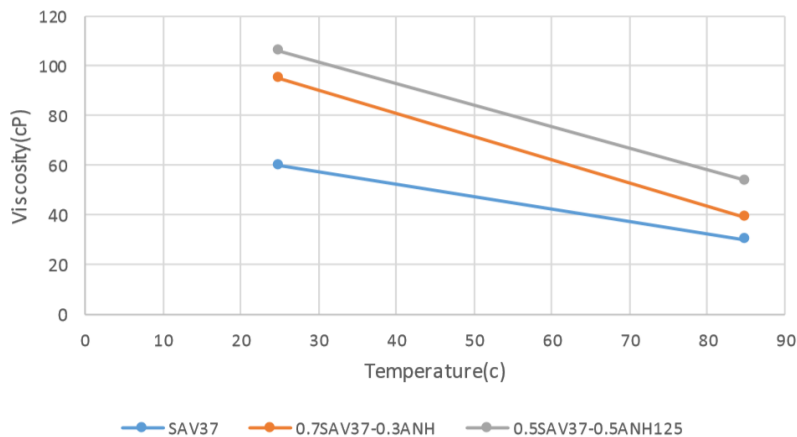


Figure 22- Thermal stability of polymer solutions in salinity in salinity of 150000 ppm

Finally, **Ошибка! Источник ссылки не найден.**²³ and ²⁴ represents the results of core flooding experiment. The same composition of polymers was used in this test as in the long-term thermal stability experiment. Clearly, performance of the polymer flooding was almost twice as better as that of the water flooding, accounting for 52% and 30% in total oil recovery, respectively. Subsequently, Application of polymer flooding demonstrated much better result in decreasing of residual oil saturation than water flooding (see Figure 24).

The results of this work showed that the combination of the functional group provides good thermal and salinity tolerance. The investigated polymer solution had an appropriate performance in conditions, which were more hostile than that of the Uzen field. Thus, co and terpolymer containing ATBS and/or NVP groups can be possible candidates with proper stability and displacement efficiency for the application in the Uzen field.

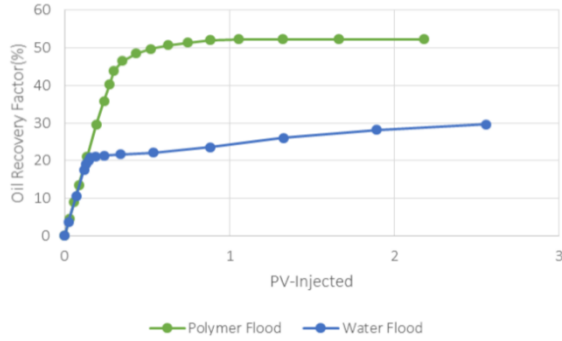


Figure 23 - Oil recovery factor vs. PV injected curves for two flooding regimes (confining pressure – 2000 psi, temperature – 85 °C, salinity level – 10000 ppm)

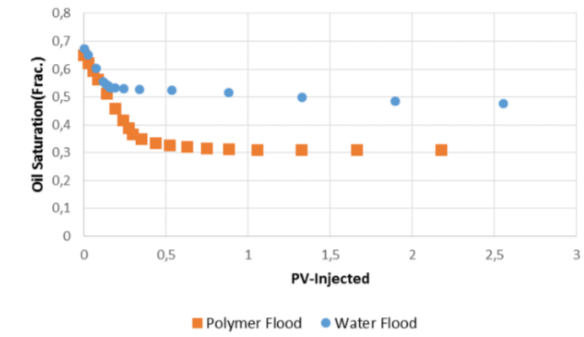


Figure 24 - Oil saturation vs PV injected curves for two flooding regimes (confining pressure – 2000 psi, temperature – 85 °C, salinity level – 10000 ppm)

2.5.3. The bulk scale investigation of 9 synthetic ATBS and NVP containing polymers.

Authors of this work performed a series of laboratory bulk scale experiments to investigate stability of 9 synthetic polymers with NVP and ATBS monomers in the functional group. The temperature of experiments varied from 70 to 140 °C, which is higher than reservoir temperature of the Uzen field. However, the aim of this study was to compare polymer performance in a very low and high salinity environment. This work can be used in the selection of polymers functional group, which can be tolerant to a specific condition. Thus, the paper can be a good guide for the screening of proper polymer for the application in the Uzen field.

Table 10 provides the list of polymers, which were used in the investigation and molecular weights. Polymers are listed by increasing of ATBS monomer content in the structure from top to bottom. In addition, all terpolymers contain NVP monomer.

Table 10 - Composition of polymers

| Product | Polymer type | M _w , million Daltons |
|---------------------|--------------|----------------------------------|
| Flopaam™ AN110VHM | Copolymer | 10–12 |
| Flopaam™ 5115VHM | Terpolymer | 14–15 |
| Flopaam™ 5220VHM | Terpolymer | 12–14 |
| Superpusher™ SAV226 | Terpolymer | 3–5 |
| Flopaam™ AN125VHM | Copolymer | 10–12 |
| Flopaam™ AN132VHM | Copolymer | 9–11 |
| Superpusher™ SAV333 | Terpolymer | 3–5 |
| Superpusher™ SAV55 | Copolymer | 5–7 |
| Superpusher™ SAV37 | Copolymer | 4–6 |

Polymers with the low content of ATBS monomers from the Table 10 was chosen for the first experiment. The long-term thermal stability tests in the salinity of 98000 ppm and temperature of 70 °C showed that all polymers were stable over 1 year period (see Figure 25). As a result, the increase in level of ATBS content provided polymers with better viscosifying ability at the same environment.

Generally, ATBS-containing polymers are capable to retain their properties at 70 °C. Therefore, authors conducted the same experiment but in more hostile environment as illustrated on Figures 26 and 27. Temperatures were the same and salinity level of the first experiment constituted 56000 ppm, while solutions for the second experiment were prepared at the same salinity level as in previous test. Significantly, the increase in the salinity levels affected the performance of the same polymers by reducing their viscosities. Flopaam™ AN110VHM was replaced by NVP-containing Sav226 terpolymer in the test with a higher salinity to evaluate the effect of NVP group on the stability of polymer. The presence of this monomer allowed terpolymer to be stable for 1 year period in contrast to performance of copolymers.

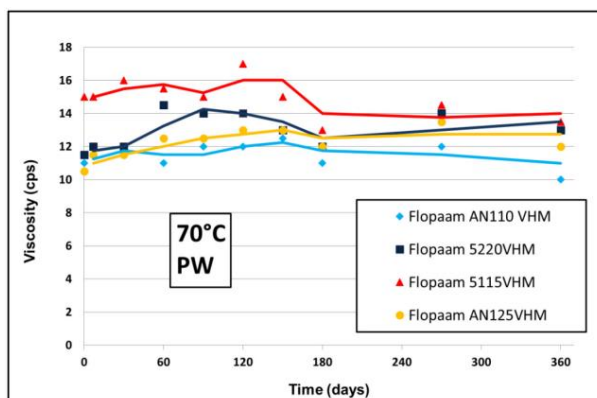


Figure 25 - Long-term thermal stability polymers from low to medium level of ATBS content at the salinity level of 98000 ppm and polymer concentration of 1500 ppm

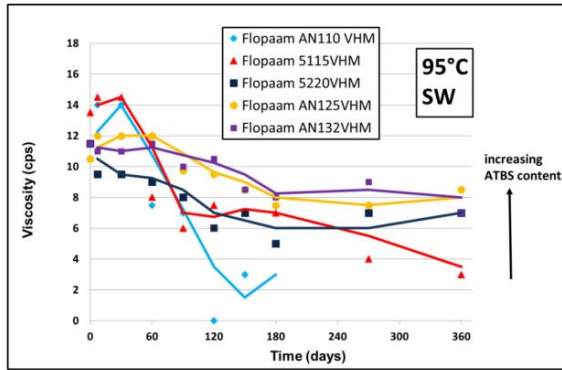


Figure 26 - Long-term thermal stability of polymers at the salinity level of 56000 ppm and polymer concentration of 1500 ppm

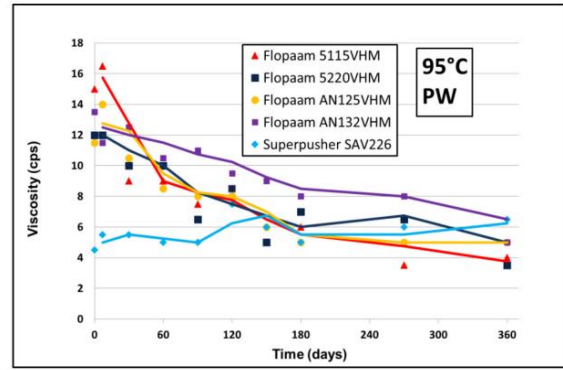


Figure 27 - Long-term thermal stability of polymers at the salinity level of 98000 ppm and polymer concentration of 1500 ppm (Sav226 – 2000 ppm)

Thus, based on results authors recommended a guide for a selection of polymers by a specific conditions of the Field. However, it is necessary to conduct first a oil displacement and injectivity tests with a core flooding experiments to see the big picture. According to Figure 28, the proper candidate for the application in the Uzen field should a polymer with high ATBS content such as AN132VHM and Superpusher Sav55.

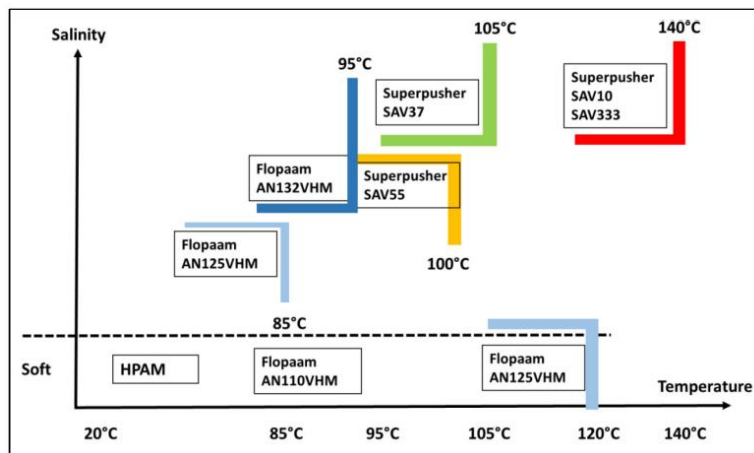


Figure 28 - The guidance of polymer selection based on salinity and temperature.

2.5.4. Comparative analysis of polymer flooding using polysaccharides and a synthetic polymer under harsh conditions (Liang et al., 2019)

The various laboratory experiments were conducted for the comparison of polymer stability under the varied temperature and salinity level. Namely, traditional EOR grade polymer, HPAM, and three biopolymers were investigated. These are Scleroglucan, Diutan gum and Xanthan gum. Chemical structures of these polysaccharides are given in **Ошибка! Источник ссылки не найден.29**.

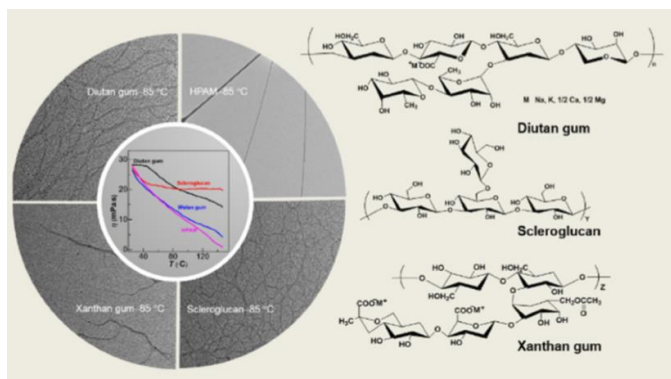


Figure 29 – The chemical structures of investigated polymers

A core was prepared from consolidated sand, with 2.5 cm of diameter and 30 cm of length. With a permeability range from 270-365, which is reference to permeability of TS-1 and TS-2 regions in the Uzen field. Porosity range of cores was 20.6 – 23.4, which is in the target range. Two types of brine solution with different compositions were synthesized. The first one contained only NaCl with different level of salinity. The second one consisted of NaCl, CaCl₂ and NaN₃.

First, authors investigated temperature effect on polymer solutions (see Figure 300). Transmission electron microscopy (TEM) combined with rheological tests were used to determine the effect of temperature. Different concentrations of polymers were used for this test. The HPAM solution degraded the most (1 cp at 150 °C), while Diutan gum with roughly same concentration showed much better performance with 25 cp at the same temperature. Solution with 0.25 % of scleroglucan was the most temperature tolerant in comparison to others. Solvent was pure water as ions of salt has negative effect on TEM.

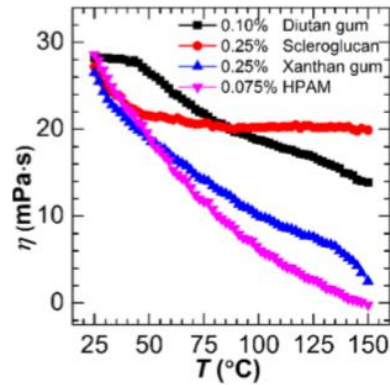


Figure 30 - Loss of apparent viscosity with increasing temperature (no salt, shear rate = 100 s^{-1}).

Next, influence of salinity variation on polymer stability was investigated as shown on Figure 31. The concentration of salt ions was increased slightly up to $20 \times 10^4 \text{ mg/L}$. Figure 312 demonstrates that, biopolymers showed much better salinity tolerance in comparison with HPAM, which experienced a dramatic decrease in apparent viscosity and resulted 1.5 cp at the maximum level of salinity. Meanwhile, insignificant viscosity loss was observed after exposure of Diutan gum and Xanthan gum to high salinity environment. Viscosity retention of these polymer solutions constituted 94.3 % and 87.2 % respectively. However, the best salinity tolerance was shown by Scleroglucan, which viscosity remained stable during the whole experiment (18 cp). This difference between stability of synthetic and biopolymer could be explained by nonionic structure of polysaccharides, which provide biopolymer with convenient salinity tolerance (Bluhm, 1982).

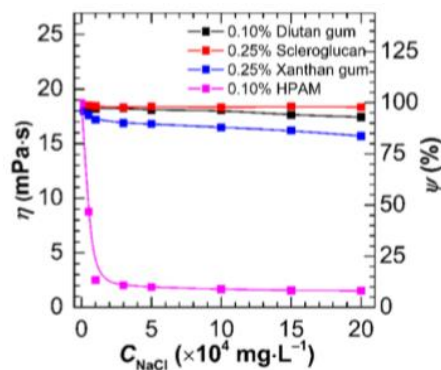


Figure 31 - Loss of apparent viscosity and viscosity retention with increasing level of salinity (temperature = $85 \text{ }^\circ\text{C}$, shear rate = 100 s^{-1}).

In the next experiment researchers studied dependence of viscosity on polymer as illustrated on Figure 32. Viscosity of biopolymer solutions reached the same values as for HPAM solution with significantly lower concentration required. Furthermore, at the same concentration of solutions, diutan gum showed viscosity values three times higher than the rest.

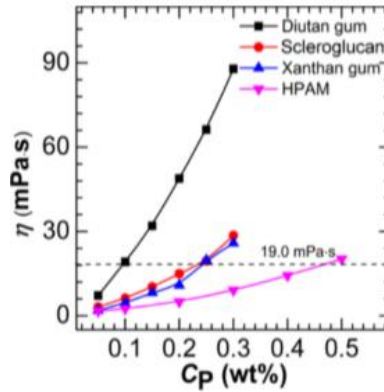


Figure 32 - Viscosity of polymer vs. concentration (temperature = 85 °C; salinity level – 10.1×10^4 mg/L).

One of the most important tests for implementation of polymer flooding is long term thermal stability. Figure 333 gives information about polymers' viscosity changes during 3 months in the hostile environment. As results show, the most stable polymers among the others were Scleroglucan and Diutan gum showing almost no viscosity loss during 90 days at harsh conditions. On the other hand, Xanthan gum and HPAM solutions experienced substantial reduction in apparent viscosity during the same time period accounting for about 3 cp at the end. This could be explained by high-rate hydrolysis of HPAM at high temperatures and disordered state of Xanthan molecules, which in both cases lead to rapid viscosity reduction (Sorbie, 2013).

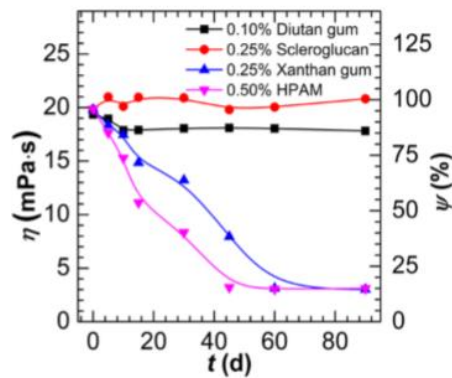


Figure 33 - Long term thermal stability test in salinity of 10.1×10^4 mg/L.

Figure 344 demonstrates change of viscous and dynamic elastic modulus with variation of frequency. A, b, c, d is for Diutan gum, Scleroglucan, Xanthan gum and HPAM, respectively. Modulus lines of the first two polysaccharides intersected at the moderate frequencies meaning that there is no critical damage to structures of these polymers was observed. Moreover, according to the experiment both solutions of Diutan gum and Scleroglucan exhibited viscoelastic properties. As a result, these polymers can be effective displacement agent as viscoelastic fluids perform higher effective viscosity with adequate decrease of permeability (Wang et al., 2001).

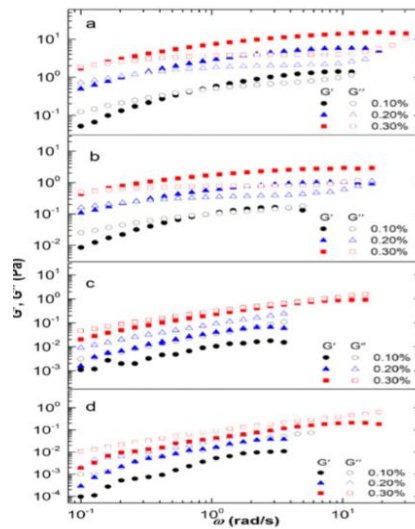


Figure 34 – Viscous modulus (G'') and dynamic elastic modulus (G') for the polymer solution (temperature = 85 °C; salinity level – 10.1×10^4 mg/L).

After rheological experiments were finished core flooding tests were designed. The table below provides data about cores and adsorption, RF and RRF of the polymer solutions. HPAM polymer solution experienced the highest adsorption of $0.177 \text{ mg} \times \text{g}^{-1}$, the next one was Xanthan gum solution. Diutan gum and Scleroglucan performed less adsorption issues. This tendency is due to increase in molecular weight. HPAM molecules has a much higher molecular weight, which leads to a greater decrease in effective porosity and therefore a greater chance of trapping compared to polysaccharides. Both RF and RRF of Diutan gum and Scleroglucan are higher than that of HPAM and xanthan gum.

Table 11 - Outcomes of the coreflooding

| core number | samples | ϕ (%) | 1 PV (mL) | K_w (mD) | η_p (mPa·s) | RF | RRF | adsorption value (mg·g ⁻¹) | η_{ef} |
|-------------|--------------|------------|-----------|------------|------------------|------|-----|--|-------------|
| 1 | diutan gum | 23.4 | 34.4 | 365 | 18.7 | 13.0 | 8.5 | 0.104 | 1.53 |
| 2 | xanthan gum | 20.6 | 30.3 | 271 | 19.2 | 7.9 | 5.6 | 0.152 | 1.41 |
| 3 | HPAM | 22.1 | 32.5 | 340 | 19.1 | 8.7 | 6.4 | 0.177 | 1.35 |
| 4 | scleroglucan | 21.1 | 31.1 | 303 | 19.2 | 10.6 | 7.1 | 0.127 | 1.49 |

Figure 35 displays pressure drop and recovery factor, which were reported during core flooding under HTHS environment. The slight difference in recovery factors between polymer solutions is observed. However, the combination of these results and data which are shown on Figure 33 gives a clear picture about unsuitability of HPAM and Xanthan gum solution for application in fields with the hostile environment, which was simulated in this work.

This work showed that biopolymer exhibits less adsorption with a suitable RF and RRF. Therefore, biopolymers can be applied as a potential candidate in the Uzen field.

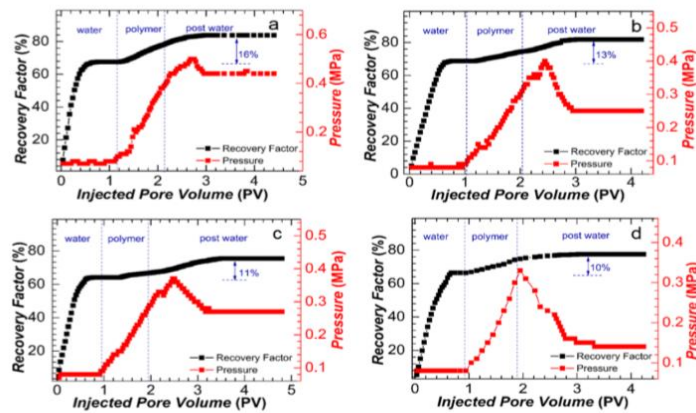


Figure 35 - Pressure drop and Recovery factor vs. Injected PV (temperature = 85 °C; salinity level – 10.1×10^4 mg/L) (A, b, c, d is for Diutan gum, Scleroglucan, Xanthan gum and HPAM respectively)

3. Methodology

A successful field implementation of polymer flooding requires a set of well-designed laboratory experiments. This thesis work was designed to evaluate performance of three synthetic polymers under reservoir conditions of the Uzen field. Consequently, outcomes of this work can be used for a further

Reservoir data of the Uzen field from the Literature review, was used in laboratory experiments, which are described in this section. Screening of the suitable polymer and its optimum concentration for a certain field, based on complex analysis of formation data, requires a well-designed set of laboratory experiments. Potential candidates for application in field conditions must meet several screening criteria. Particularly, target polymer solution must maintain required viscosifying ability under Uzen field's reservoir conditions for a sufficient period of time. Furthermore, the polymer has to provide acceptable injectivity results and displacement efficiency. Thus, a series of laboratory tests were designed and conducted to investigate performance of several polymer solutions with different concentrations:

- Bulk scale rheological analysis of polymer solutions at varying conditions allowed to determine desirable concentrations for each of the chosen polymers. Particularly, the effect of concentration and temperature on viscosity of polymer were studied.
- Investigation of mechanical degradation showed the ability of polymers to maintain viscosifying abilities under high shear rate conditions, which could arise at certain points such as perforations in the field conditions.
- A long-term thermal stability experiment is required to study the viscosity retention of polymers under reservoir temperature for a long period of time.
- Injectivity tests on core flooding system was designed to evaluate several factors. Firstly, the permeability reduction of porous media was estimated. Secondly, the target polymer must provide minimum pressure drop while being injected to the formation for more efficient displacement (Seright et al., 2009). The last factor to study is the viscosity loss of polymer solutions during the injection to sandstone rock.

- Oil displacement test was set up to evaluate the oil recovery by selected polymer during core scale polymer flooding.

Figure 36 shows a flowchart of polymer screening process. More information will be provided in the following sections.

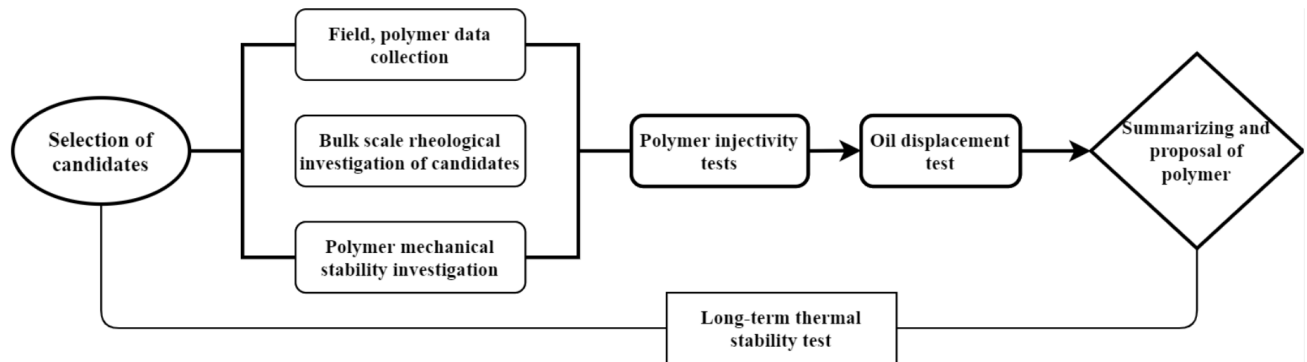


Figure 36 - Flowchart of polymer screening process

3.1. Materials

The information about materials such as the formation water, polymers, core and oil samples are presented in this subsection.

3.1.1. Formation water:

Uzen formation water was synthesized based on data from open sources (Mullayev et al. 2017). The concentration of TDS was 77000 ppm. Table 12 gives information about ion composition and mass of salts, which were used for synthesis.

Table 12 - Ion composition and mass of salts for Uzen field formation water

| Ion | Concentration, ppm |
|-----------|--------------------|
| Na^+ | 23430 |
| Ca^{2+} | 4450 |
| Mg^{2+} | 1300 |
| Cl^- | 47780 |

| Salt | Mass, g |
|---|---------|
| <i>NaCl</i> | 59.55 |
| <i>MgCl₂.6H₂O</i> | 10.86 |
| <i>CaCl₂.2H₂O</i> | 12.32 |

3.1.2. Oil sample

Oil, which was used as a reference displaced fluid in core flooding experiments, was arrived from Kenkiyak-Kumkol field. Unfortunately, the use of oil from the Uzen field was not possible due to inaccessibility of samples at the time of the experiments. Nevertheless, the viscosity of the oil samples, which was used in this work lower than the actual one by 1.5 to 2 cp in the conditions of Uzen field. The oil viscosity at room and reservoir temperature are shown in Table 13. Figure 37 presents the filtered oil sample, which was used in the displacement experiment.

Table 13 - Reference oil viscosity

| Temperature, c° | Viscosity, cp |
|-----------------|---------------|
| 20 | 5.80 |
| 60 | 2.38 |



Figure 37 - Crude, filtered oil from Aktobe

3.1.3. Rock sample

Berea sandstone cores were used as a reference reservoir rock for the core-flooding experiments. Figure 38 shows 3 cut core samples. Porosity and permeability range of Berea sandstone are similar to that the Uzen formation's TS-3 and TS-2 regions. This range was used in this work as the worst case scenario.



Figure 38 - Berea sandstone core samples and powder

3.1.4. Polymers

Sav 10, Sav 19 and Sav 10 XV Superpushers were studied in this work. These are commercially available water-soluble polymers, which were provided by SNF Floerger. All of them are copolymers with two functional groups (see Figure 39).

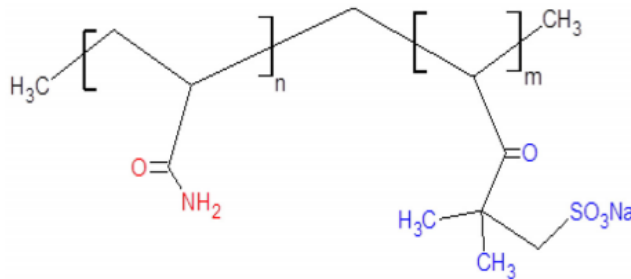


Figure 39 - General structure of investigated polymers (Quadri, 2015)

The studied polymers have the same chemical structure and contain acrylamide (AM), acrylamido-tert-butyl sulfonate (ATBS). The only difference between them is molecular weight. The polymer with the highest molecular weight is Sav 10 XV, the second highest is Sav 19, and

Sav 10 is the lightest among them. Polymers are provided in the form of powder. Figure 40 shows polymer sample in beakers.



Figure 40 - Polymer samples

3.2. Experimental methods and procedure

3.2.1. Brine and polymer solutions preparation procedure

The composition of 16th horizon of Uzen field was used for the preparation of polymer solution as a make-up water and injection water in core flooding experiments. The make-up brine solution was prepared by continuous mixing of salts, which were weighed according to the Table 12 on a magnetic stirrer.

After 77000 ppm brine solution is ready, polymer solutions were prepared as per standards of API (API RP 63). The make-up brine solution of required volume in a beaker was placed on magnetic stirrer to create vortex, which occupied 70% of the water volume. Next, polymer powder is weighed on a weighing scale according to the equation below:

$$W(\text{polymer}), g = \frac{C(\text{polymer}), \text{ppm} * V(\text{solution}), \text{ml}}{10^6} \quad (1)$$

After that, a polymer powder was slowly sprinkled on the shoulder of the vortex over 30 seconds to avoid forming of large slug of polymer powder. The solution was covered with parafilm and stirred for about 3 hours with the rotation rate of 80-100 rpm on a magnetic stirrer.

3.2.2. Bulk scale rheological investigation

The first step in screening of suitable candidate was to investigate the rheology of candidates. The effects of temperature and concentration on the rheology provides an initial understanding to the properties of polymers. It is crucial to know the behavior of polymer's rheology at different temperatures as it might vary in different regions of the reservoir. The highest viscosity value at the same polymer concentration among three Superpushers was measured as well. This value of viscosity should be demonstrated by polymer with the highest molecular weight. The salinity level of Uzen formation water for polymer solutions preparation was used in all cases. Thus, this investigation was mainly focused on the effects of temperature, concentration, and shear rate.

Figure 41 represents the Modular Compact Rheometer (MCR), which was used for rheological investigations at the bulk scale. Two measuring systems were used to measure the viscosity of polymers as a function of shear rate at different stages of laboratory experiments.

Preliminary analysis was required to study the effect of temperature and concentration variation on polymers performance and to design further experiments properly. The effect of temperature and concentration variation was investigated using a cylindrical measuring system (see Figure 43). The temperature was gradually increased from 25 C° to 80 C°, while concentrations of polymers varied from 1500 to 3000 ppm.

The evaluation of polymer viscosity at room temperature was conducted using a cone plate measuring system (see Figure 42). The volume of sample required for the system is about 1.5 ml, which is suitable for tests with low volume of samples such as long-term thermal stability, mechanical stability experiments and effluents viscosity determination.



Figure 41 - Anton Paar MCR 301 Rheometer



Figure 42 - Cone plate Measuring System for the MCR



Figure 43 - Cylindrical Measuring System for the MCR

3.2.3. Long-term thermal stability tests

The long-term thermal stability test was designed to evaluate the ability of polymers solutions to maintain the viscosity under high temperature conditions. 2500 ppm of each polymer was poured into 25 test tubes and placed into the oven with the temperature of 80 C° and oxygen-free environment. Each test tube was labeled with the date of experiment. The duration of the experiment was 60 days. After certain amount of time test tubes were moved out of the oven for the viscosity measurement.

3.2.4. Mechanical degradation

Mechanical stability of the chosen polymer solutions was evaluated using Hamilton Beach Single Spindle Drink Mixer HMD 200 (Figure 44). 3 polymer solutions with 2500 ppm polymer concentration were exposed to high shear rate of 400 s⁻¹ for different time intervals. Viscosity retention was measured at room temperature and 10.8 1/s shear rate after 0, 1, 2, 3, 4, 5, and 10 minutes of exposure to a high shear rate. Viscosity values and degree of degradation (DR) were calculated as well.

$$DR = \frac{\mu_{initial} - \mu_{after\ test}}{\mu_{initial}} \quad (2)$$



Figure 44 - Hamilton Beach Single Spindle Drink Mixer HMD 200

3.2.5. Core preparation

Berea sandstone core were used in the core flooding experiments. 4 core plug samples with diameter of 1.5 inch were cut into length of approximately 3 inches. These samples were placed into the oven at 80 °C over night. Core samples were then saturated with formation water of Uzen field under 1000 psi. A core saturator, which is shown on Figure 45 was used for this purpose. Physical properties measurements were carried out in the core preparation process.



Figure 45 - Core saturator

3.2.6. Injectivity tests

The core-flooding experiments were conducted to estimate injectivity and polymer retention in porous media. The retention of polymer solution in the rock causes permeability reduction (Seright et al., 2009). It can be quantitatively expressed in terms of resistance factor (RF) and residual

resistance factor (RRF) (Hincapie 2016). RF represents the ability of polymer to control the mobility and defines as:

$$RF = \frac{\Delta P(\text{polymer injection})}{\Delta P(\text{brine injection before polymer injection})} \quad (3)$$

RRF shows the effect of polymer retention and permeability of porous media and defines as:

$$RRF = \frac{\Delta P(\text{brine injection after polymer injection})}{\Delta P(\text{brine injection before polymer injection})} \quad (4)$$

RF and RRF values were calculated at steady state flow.

For this experiment, 3 core samples were prepared, and 3 concentrations of each polymer were injected into each core. Table 14 shows viscosities of the chosen polymer solutions at room and reservoirs temperature before the injection. The brine was injected before and after each polymer. The core flooding system (Figure 46) was used to perform injectivity test at confining pressure of 1000 psi (2000 psi for Sav 10 XV), and temperature of 60 C°. All polymer solutions except Sav 10 XV with 1000 ppm of polymer concentration were injected with 5 different rates of 0.5, 1, 1.5, 2, 5 cc/min.



Figure 46 - Core-flooding apparatus

The effluent samples were collected at each rate for every polymer concentration to estimate polymer degradation after the flooding.

Core absolute brine permeability was calculated by the following formula:

$$K_{abs} = \frac{14700 \cdot q \cdot \mu \cdot L}{A \cdot \Delta P} \quad (5)$$

Table 14 - Initial viscosities of polymer solutions

| Polymer solution | Viscosity at room temperature and 10.8 s ⁻¹ , cp | Viscosity at reservoir temperature and 10.8 s ⁻¹ , cp |
|--------------------|---|--|
| Sav 10 2500 ppm | 8.15 | 5.52 |
| Sav 10 1250 ppm | 4.61 | 3.26 |
| Sav 10 625 ppm | 2.35 | 1.63 |
| Sav 19 1800 ppm | 7.07 | 4.57 |
| Sav 19 900 ppm | 3.12 | 1.89 |
| Sav 19 450 ppm | 2.21 | 1.30 |
| Sav 10 XV 1000 ppm | 4.96 | 3.63 |
| Sav 10 XV 500 ppm | 2.63 | 1.93 |
| Sav 10 XV 250 ppm | 1.31 | 0.94 |

3.2.7. Oil Displacement test

After all previous laboratory investigations were completed, the potential polymer for application on Uzen field was selected for oil displacement test. Determination of displacement efficiency in terms of recovery factor is mandatory stage of polymer screening. With that in mind, core-scale polymer injection into the sandstone rock was designed and implemented. Figure 47 represents the sequence of the tests.



Figure 47 - Oil displacement test sequence

The experiment was conducted at confining pressure of 1000 psi, and reservoir temperature of 60 C°. Brine and polymer solutions for oil recovery were injected at rates of 0.5, 1, 2, and 5 cc/min. The procedure of in-situ and effluents viscosity calculations was the same as in subsection 1.2.6.

4. Results

This section includes the description of results and discussion of experiments discussed in the previous chapter. The whole set of laboratory investigations helped to screen and determine suitable polymer for the application in Uzen field. All measurements and experiments were conducted at the same operational conditions for all polymer solutions. To screen the most appropriate polymer, the following criteria were considered for the evaluation:

- the highest viscosifying ability at the same concentration
- stability of polymer in terms of viscosity retention after exposure to high shear rate
- acceptable viscosity reduction (less than 50%) during long-term exposure to high temperature
- the best injectivity and the lowest differential pressure during injection to the sandstone core
- the appropriate oil displacement and oil recovery by the selected polymer after waterflooding

4.1. Bulk scale rheological investigation

This subsection describes the rheological behavior of polymers at different temperatures and concentrations. Generally, all the investigated polymers showed similar to polymers from analogy review section behavior with increase in temperature and concentration.

4.1.1. The effect of concentration.

A polymer concentration is in direct proportion to viscosity. Increase in concentration led to significant growth of viscosity values in all cases as given on Figures 48-50 and Table 15. The temperature of the measurements was 60 °C, which is approximately equal to that of Uzen field. Considering results, the most viscous polymer at equal concentrations among three Superpushers was Sav 10 XV in all cases. It can be explained by the higher molecular weight of this polymer as all of them have the same chemical structure. Nevertheless, Sav 10 and Sav 19 was less shear

sensitive, which was evident from Figure 52. Comparing to Sav 10 XV, these polymers showed a less significant decrease in viscosity with increase in shear rate at all concentrations.

All polymer solutions demonstrated a non-Newtonian shear thinning behavior with an increase in shear rate as well as all polymer from analogy evaluation section. However, the Sav 10 XV exhibited typical a small Newtonian fluid region at the higher shear rates as shown on Figure 50.

Table 15 - Viscosities of polymers solution at different concentrations, temperature of 60 °C, and shear rate of 10.8 s⁻¹

| Polymer solution | Polymer | | |
|--|---------|--------|-----------|
| | Sav 10 | Sav 19 | Sav 10 XV |
| Viscosities at 1500 ppm polymer concentrations, cp | 2.78 | 3.81 | 6.10 |
| Viscosities at 2500 ppm polymer concentrations, cp | 4.30 | 6.70 | 10.28 |
| Viscosities at 3000 ppm polymer concentrations, cp | 6.25 | 12.66 | 13.71 |

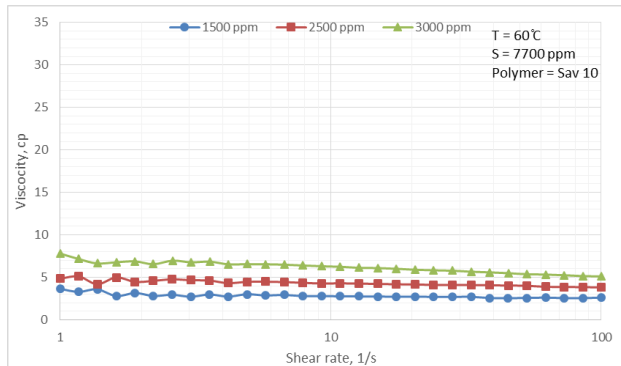


Figure 48 - The effect of concentration and shear rate on rheological behavior and viscosity of Sav 10

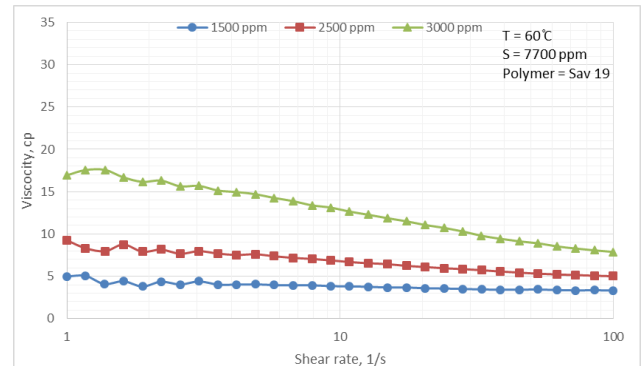


Figure 49 - The effect of concentration and shear rate on rheological behavior and viscosity of Sav 19

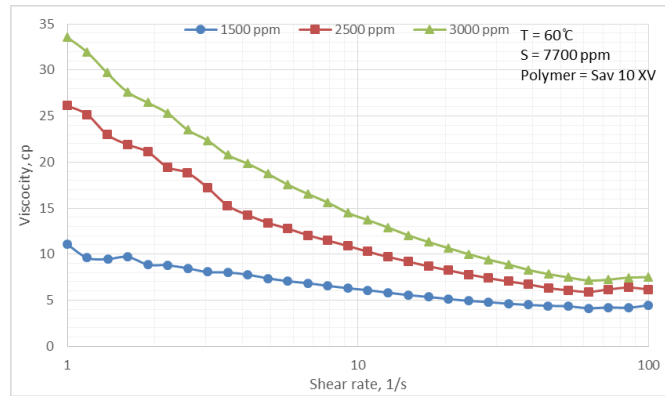


Figure 50 - The effect of concentration and shear rate on rheological behavior and viscosity of Sav 10 XV

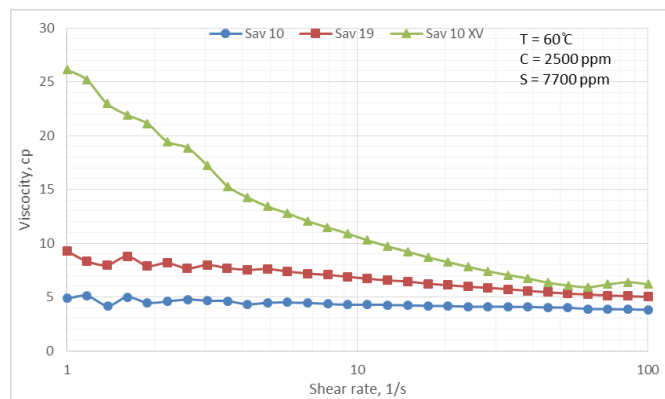


Figure 51 - Rheological comparison of polymers with increase in shear rate at the same polymer concentration

4.1.2. The effect of temperature

The effect of temperature on viscosities of Superpushers is shown on Figure 52-60. Change of viscosity values with increase in temperature and shear rate is given on semi log plots. The description and interpretation of results in this section are valid for all polymer concentrations. All three polymers demonstrated behavior of non-Newtonian shear-thinning fluids with an increase in shear rate and temperature. Moreover, Sav 10 XV showed more shear sensitive behavior with a dramatic viscosity loss compared to other two polymers in all cases. In addition, Newtonian fluid behavior of Sav 10 XV solution was observed at the higher shear rates.

The elevation of the temperature to 80 °C decreased initial values of viscosities of all solutions by a half. Thermal degradation factors were calculated to show the degree of elevated temperature effect on viscosity decrease. Figure 61 represents thermal degradation degree of all three polymers.

Clearly, 2500 ppm Sav 10 solution has the worst thermal stability with roughly 60 % of viscosity loss at 80 °C. Nevertheless, viscosity values did not fall below half the initial value for all other polymer solutions, including the two remaining Sav 10 concentrations. Generally, these values were acceptable for further screening especially as temperature degradation factor did not exceed 38 % for 60 °C, which is the reservoir temperature of Uzen field. Thus, all polymer were able to retain the target 50% of initial viscosities.

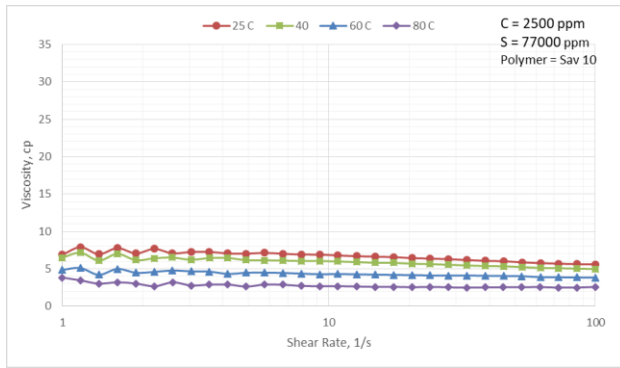


Figure 52 - The effect of temperature on rheological properties of 2500 ppm Sav 10

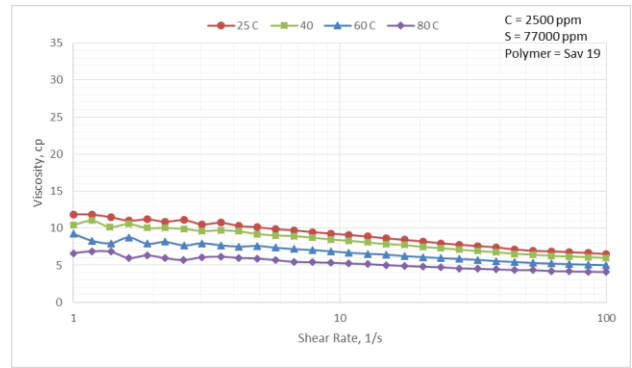


Figure 53 - The effect of temperature on rheological properties of 2500 ppm Sav 19

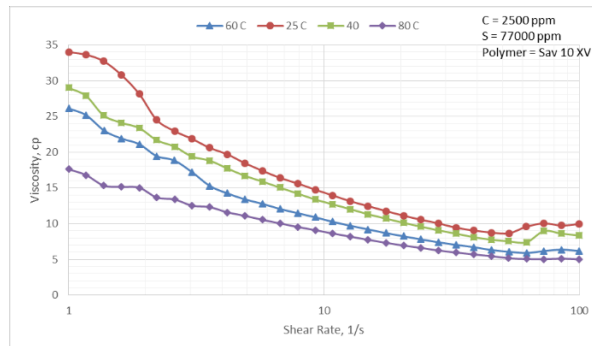


Figure 54 - The effect of temperature on rheological properties of 2500 ppm Sav 10 XV

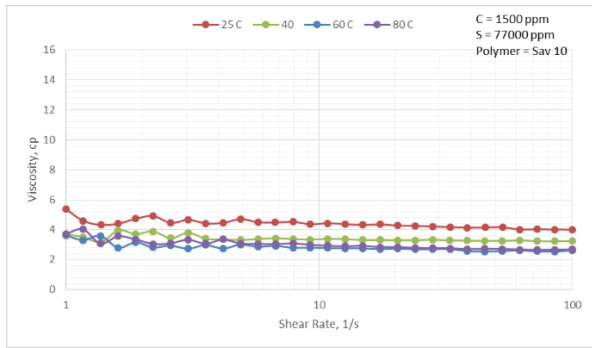


Figure 55 - The effect of temperature on rheological properties of 1500 ppm Sav 10

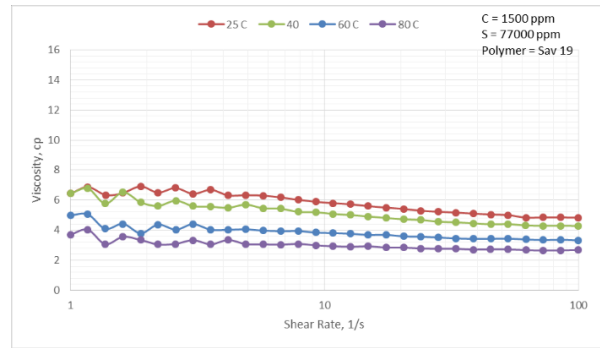


Figure 56 - The effect of temperature on rheological properties of 1500 ppm Sav 19

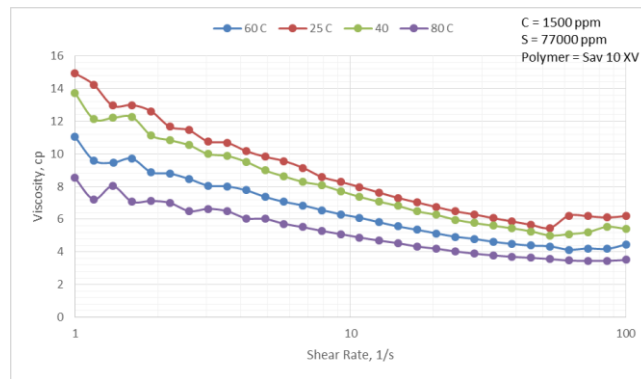


Figure 57 - The effect of temperature on rheological properties of 1500 ppm Sav 10 XV

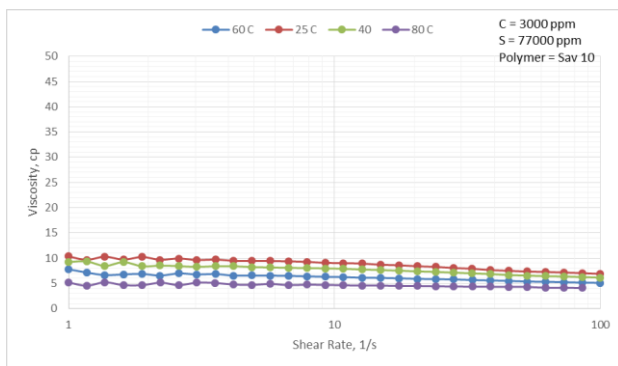


Figure 58 - The effect of temperature on rheological properties of 3000 ppm Sav 10

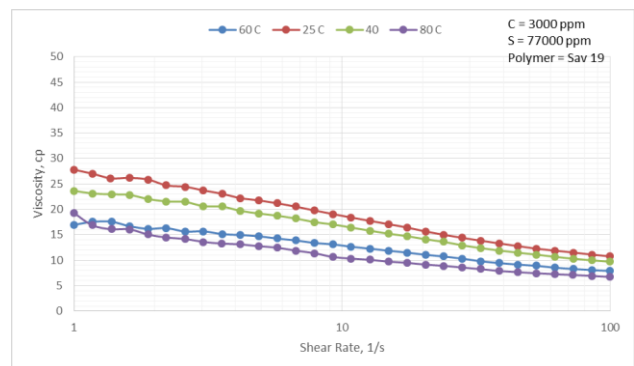


Figure 59 - The effect of temperature on rheological properties of 3000 ppm Sav 19

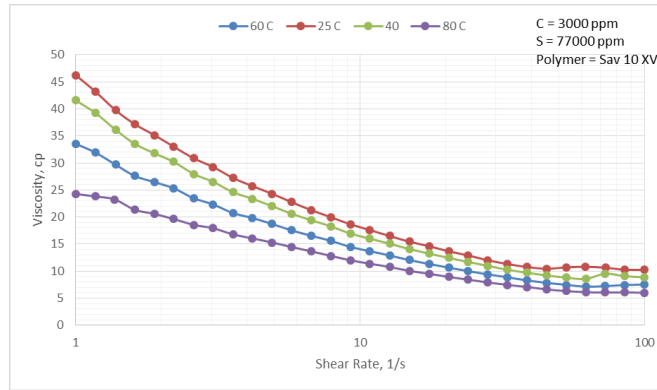


Figure 60 - The effect of temperature on rheological properties of 3000 ppm Sav 10 XV

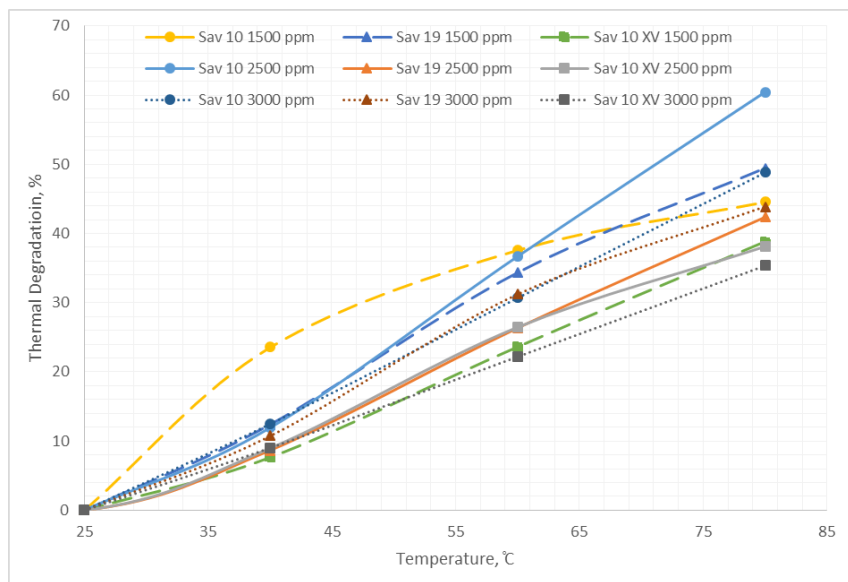


Figure 61 - Thermal degradation of the polymers

4.2. Mechanical stability

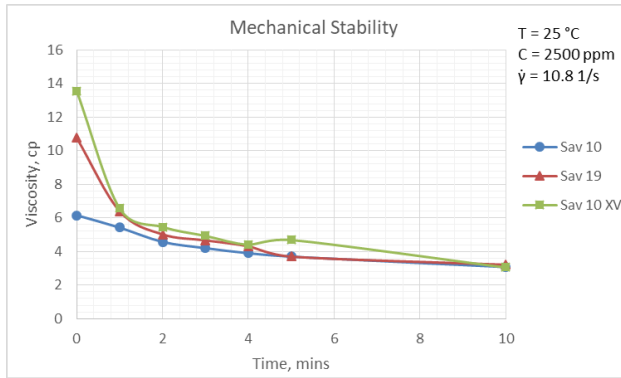
Figures 62a and 62b shows viscosity degradation of the investigated polymers during different period of time at high shear rate conditions for polymer concentration of 1500 and 2500 ppm respectively. The viscosity measurements were conducted at 10.8 1/s shear rate and room temperature for all solutions.

It is clearly seen from the graphs that, the most significant viscosity drop of all polymers occurred during the first minute of the experiment. Moreover, viscosity values became almost the same in

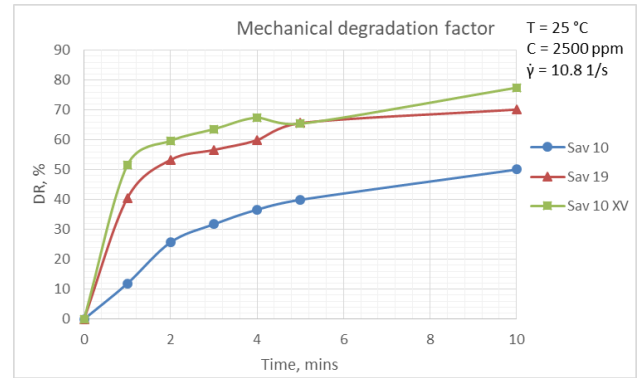
all cases after one minute of exposure to high shear rate. The subsequent viscosity degradation showed a similar tendency for all polymers up to the end of the experiment. Sav 19 and Sav 10 XV demonstrated a dramatic decrease in the viscosity after one minute of exposure to 23900 rpm compared to a gradual viscosity loss of Sav 10. It can be explained by the difference in the molecular weights. Sav 10 XV with the highest molecular weight proved to be the most shear-sensitive among three polymers. The second largest viscosity loss was demonstrated by Sav 19. These observations are valid for both polymer concentrations. Table 16 gives information about the mechanical degradation extent and provides initial viscosity values and values, which were measured after 10 minutes of exposure to high shear rate. No change in degree of mechanical degradation was observed with an increase in concentration (see Figures 62c and 62d). Nevertheless, solutions with 2500 polymer concentration gave higher final values of viscosity comparing to 1500 ppm.

Table 16 - Viscosity values and degree of degradation of polymers.

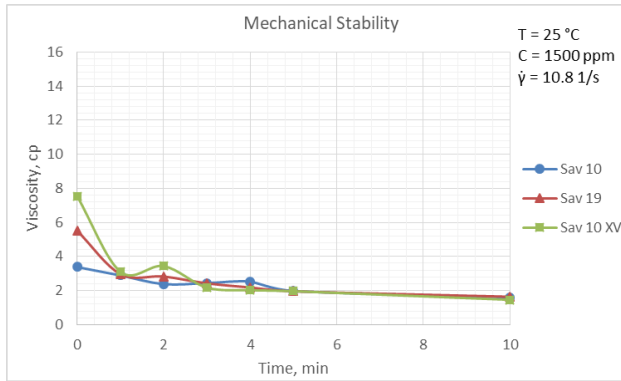
| Polymer | Concentration | | | | | |
|-----------|---------------|-----------------------------------|--------|--------------|-----------------------------------|--------|
| | 1500 ppm | | | 2500 ppm | | |
| | μ_0 , cp | $\mu_{(after\ 10\ minutes)}$, cp | DR (%) | μ_0 , cp | $\mu_{(after\ 10\ minutes)}$, cp | DR (%) |
| Sav 10 | 3.38 | 1.60 | 53 | 6.16 | 3.08 | 50 |
| Sav 19 | 5.51 | 1.64 | 70 | 10.76 | 3.21 | 70 |
| Sav 10 XV | 7.54 | 1.46 | 81 | 13.55 | 3.05 | 78 |



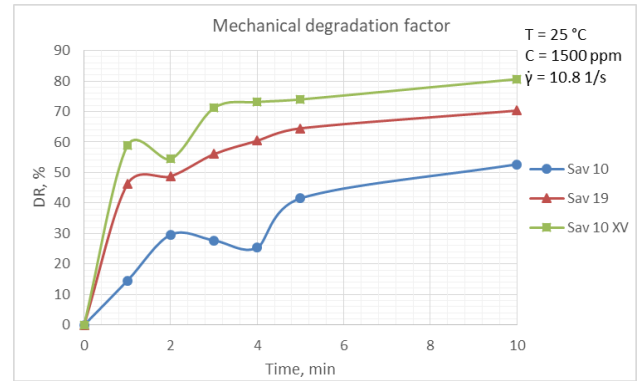
a)



c)



b)



d)

Figure 62 : a - Mechanical degradation of 2500 ppm polymer solutions during different time interval; b -Mechanical degradation of 1500 ppm polymer solutions during different time interval; c - Mechanical degradation factor of 2500 ppm polymer solutions during different time interval.; d - Mechanical degradation factor of 2500 ppm polymer solutions during different time interval.

4.3. Long-term thermal stability test

The thermal stability over significant period of time was investigated for the completion of polymer screening. Figure 63 and 64 demonstrate the results of long-term thermal stability experiment. All three candidates did not lose more than 50% of initial viscosities for 60 days exposure to 80 °C in the salinity level of Uzen formation water. Furthermore, Sav 10 XV had a viscosity degradation factor of roughly 23 % percent at the end of the experiment. According to Ham et al. (2014), the appropriate candidate for the polymer flooding must retain at least half of its initial viscosity for a long period of time in the reservoir condition.

Thus, all three polymers can be stable under conditions of Uzen field temperature, which is twenty degrees below the experimental temperature.

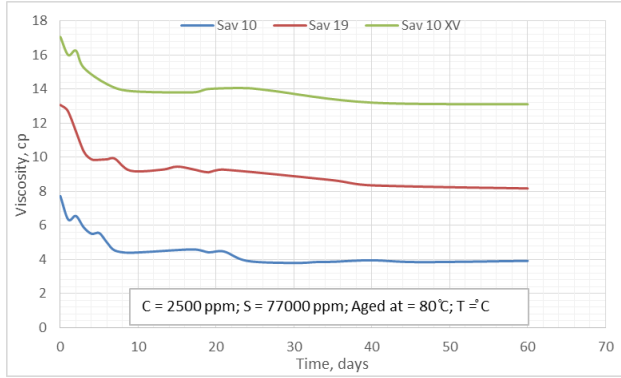


Figure 63 - Polymers' viscosity loss during 60 days at 80°C

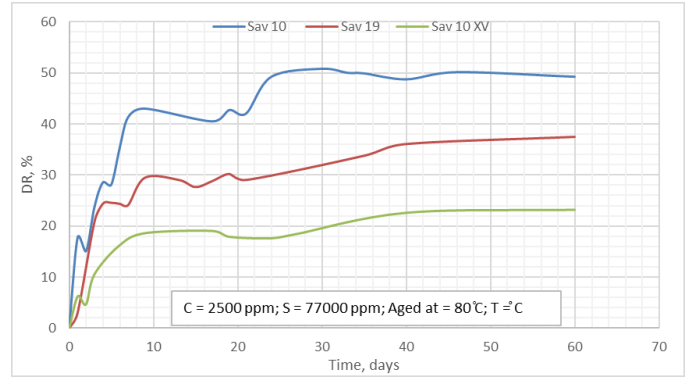


Figure 64 - Viscosity degradation degree during 60 days at 80°C

4.4. Injectivity tests

Table 17 provides calculated values of brine absolute permeabilities, RRF, and measured physical parameters of cores, which were used in injectivity tests. Firstly, pre-flush with brine flooding was conducted at each Berea sandstone core to determine absolute permeabilities of cores followed by polymers injection at different rates. As for the brine absolute permeability, it varied from 20 to 83 mD. According to the Literature Review section, these values are in the acceptable range for polymer flooding. The obtained RRF values suggest that, injection of Sav 19 polymer caused the most significant permeability reduction among three candidates even though it was injected in the core with the highest permeability values.

As expected, RF values increased with increasing molecular weight and concentration, which can be observed from Figure 65. Generally, resistance factor of all solutions increased up to 2 cc/min of injection rate due the shear-thickening effect in porous media, while it decreased at the highest rate due to severe shear-thinning. The exception is Sav 10, RF of which continued to growth even when injection rate was increased to 5 cc/min. It can be explained by less shear-sensitivity of Sav 10 comparing to other two candidates. According to Quadri (2015), there is the difference between shear rates in high and low permeability porous media at the same flux rates. As a result, this different shear behavior of polymers can be a possible reason for elevated values of RF for Sav 10 XV flooding. It should be noted that, injection rate of 1000 ppm Sav 10 XV flooding was not increased to 5 cc/min for safety reasons as differential pressure was extremely high for

coreflooding apparatus. Thus, there is no data about value of resistance factor for 1000 ppm Sav 10 XV at 5 cc/min injection.

Table 17 - Physical properties of the sandstone core samples.

| Core sample | Length, cm | Diameter, cm | Pore volume, ml | Porosity | Brine absolute permeability, md | RRF |
|-------------------------|------------|--------------|-----------------|----------|---------------------------------|------|
| #1(Sav 10 injection) | 7.69 | 3.80 | 16.95 | 0.193 | 56.98 | 6.63 |
| #2(Sav 19 injection) | 7.66 | 3.81 | 17.14 | 0.196 | 82.86 | 9.67 |
| #3(Sav 10 XV injection) | 8.00 | 3.80 | 17.78 | 0.196 | 21.76 | 7.89 |

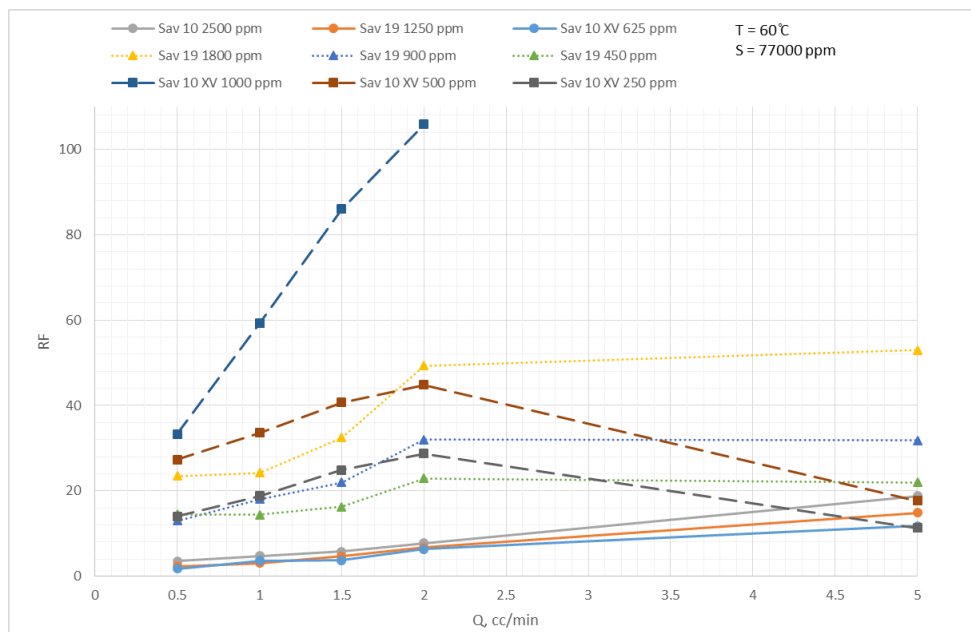


Figure 65 - Resistance factor as a function of injection rate for 9 polymer solutions.

As for the mechanical degradation of polymers in porous media, the Table 18 provides information about initial viscosity values of each polymer sample, which were made at 60 °C, and measurements of effluents viscosity, which were carried out at room temperature (after flooding at 60 °C). The viscosity degradation factor indicates that, polymer samples with higher concentration and viscosity were exposed to higher mechanical degradation. Figure 66 illustrates change of the degradation factor with an increase of injection rate. Obviously, the most substantial viscosity loss

occurred during injection at the very first rate. The subsequent degradation has been at approximately the same level.

Table 18 - Comparison of initial and effluents viscosity values with degradation factor.

| Polymer | μ_0 , cp | $\mu_{0.5}$, cp | μ_1 , cp | $\mu_{1.5}$, cp | μ_2 , cp | μ_5 , cp | DR _{final} (%) |
|----------------|--------------|------------------|--------------|------------------|--------------|--------------|-------------------------|
| Sav 10 2500 | 5.52 | 1.69 | 1.52 | 1.41 | 1.41 | 1.22 | 77.90 |
| Sav 10 1250 | 3.27 | 1.28 | 1.00 | 1.13 | 1.24 | 1.06 | 67.58 |
| Sav 10 625 | 1.63 | 1.22 | 1.22 | 1.38 | 1.25 | 0.98 | 39.88 |
| Sav 19 1800 | 4.57 | 2.31 | 2.09 | 2.01 | 1.98 | 1.95 | 57.33 |
| Sav 19 900 | 2.12 | 1.25 | 1.23 | 1.13 | 1.25 | 1.16 | 45.28 |
| Sav 19 450 | 1.30 | 1.08 | 1.00 | 1.01 | 1.11 | 1.08 | 16.92 |
| Sav 10 XV 1000 | 3.63 | 1.24 | 1.55 | 1.27 | 1.62 | - | 55.37 |
| Sav 10 XV 500 | 1.93 | 1.00 | 1.08 | 1.06 | 1.11 | 0.86 | 55.44 |
| Sav 10 XV 250 | 1.12 | 1.23 | 1.27 | 1.20 | 1.15 | 1.07 | 4.46 |

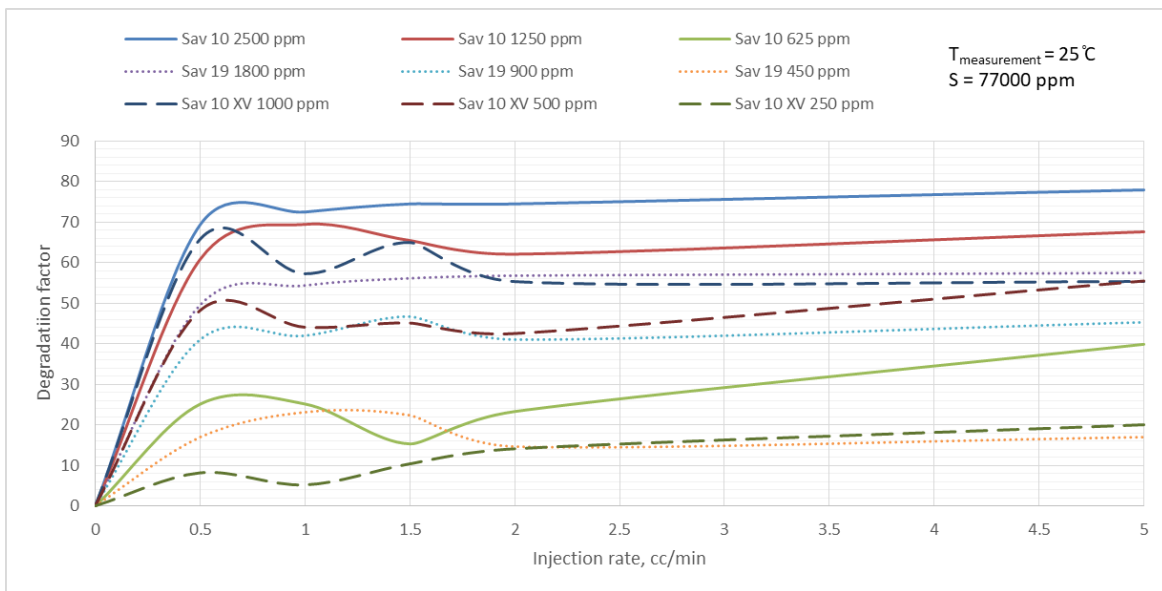


Figure 66 - Viscosity degradation factor of all polymer solutions as a function of injection rate.

The highest differential pressure at the same rates was provided by Sav 10 XV polymer solutions. All solutions of this candidate required a higher differential pressure comparing to minimum,

medium, and maximum concentrations of other two polymers. The absence of pressure data at 5 cc/min for 1000 ppm Sav 10 XV is due to the same reason as for RF. The lowest pressure values were provided by Sav 10 in all concentration groups (minimum, medium, and maximum). This contrast in pressures can be explained by the difference in the molecular weights of candidates. Results are visually represented on Figure 67.

To conclude, Sav 10 demonstrated far better injectivity at different concentrations with acceptable resistance factor in contrast to other polymers. Moreover, permeability reduction, which occurred after Sav 10 injection was the lowest among all candidates. In addition, Sav 10 polymer demonstrated the best mechanical stability at high shear rates and acceptable long-term thermal stability. Taking these factors into consideration, Sav 10 was recommended as the best choice for the follow-up displacement test.

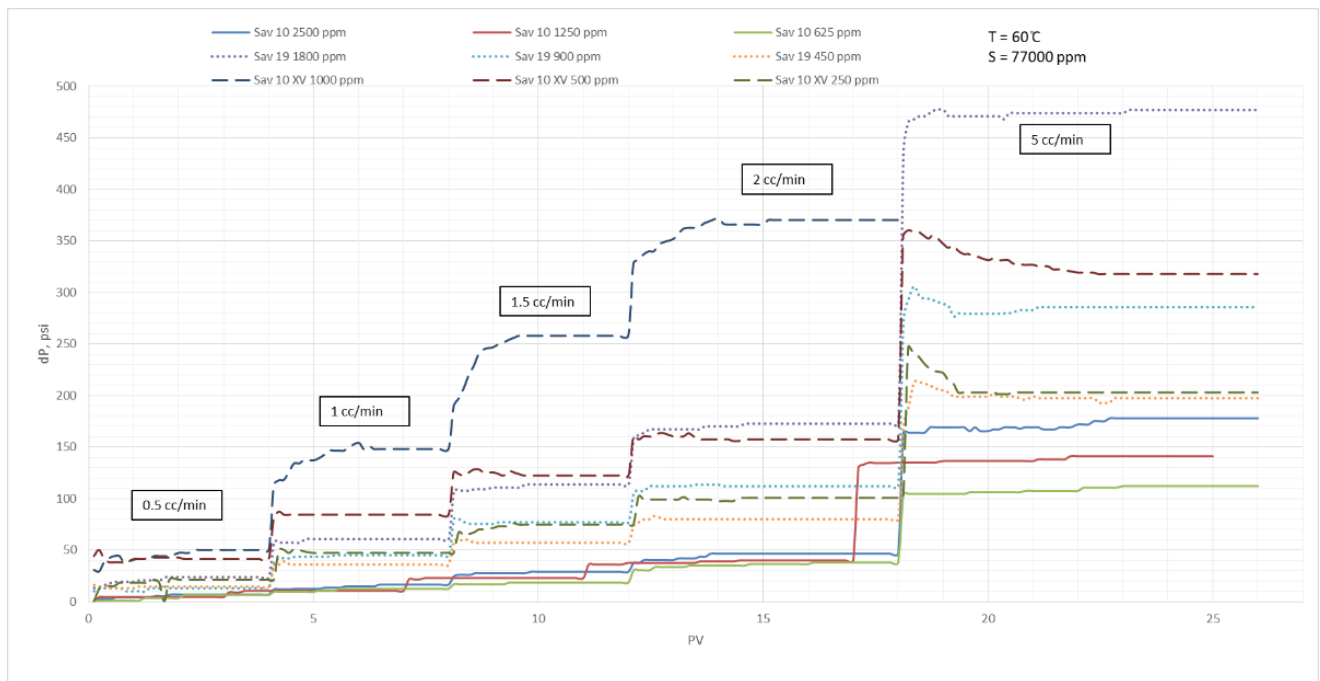


Figure 67 - Differential pressure of polymer flooding vs injected pore volume

4.5. Oil displacement test

Oil displacement test was conducted with 2500 ppm Sav 10 solution on Berea sandstone core sample. Table 19 provides petro-physical properties of the core and Table 20 summarizes several

outcomes of the experiment. Figure 68 shows the effect of application of polymer flooding on oil recovery in sandstone core sample and change in differential pressure along the displacement test.

As for in-situ rheology, viscosity degradation and resistance factors are shown on Figure 69. Polymer exhibited less mechanical degradation in comparison with performance of that solution in injectivity tests. Initial viscosity at 60 °C and viscosity of effluents after the flooding at 60 °C constituted 4.7 cp and roughly 2.35 cp respectively. Nevertheless, values of resistance factor were significantly higher than that of in injectivity test. It can be explained by the presence of displaced fluid (oil) with higher viscosity in contrast to the brine, which was used in the previous experiment. RRF value demonstrated slightly higher permeability reduction in oil displacement test because of irreducible oil saturation.

Generally, the Sav 10 injection was effective and increased total oil recovery by almost 12 % even after the oil displacement by injection of 9 PV of brine at the highest injection rate (5 cc/min). Subsequently, S_o value decreased by 8.5 % after the injection of polymer solution. To conclude, application of Sav 10 flooding improved cumulative oil recovery and can be recommended for the sector simulation.

Table 19 - Petro-physical properties of the core

| Sample | L, cm | D, cm | PV, ml | Porosity | K_{abs} (Brine), md | K_e (Oil), md | S_{wi} , % |
|----------|-------|-------|--------|----------|-----------------------|-----------------|--------------|
| Core # 4 | 7.69 | 3.80 | 17.58 | 0.20 | 90.27 | 74.74 | 28.75 |

Table 20 - Major outcomes of the oil displacement experiment

| Sample | Oil Recovery by brine flooding, % | Oil Recovery by Sav 10, % | Total Oil Recovery, % | S_o after brine flooding, % | S_o after Sav 10 flooding, % | RRF |
|----------|-----------------------------------|---------------------------|-----------------------|-------------------------------|--------------------------------|------|
| Core # 4 | 80.25 | 11.96 | 92.21 | 14.07 | 5.55 | 7.61 |

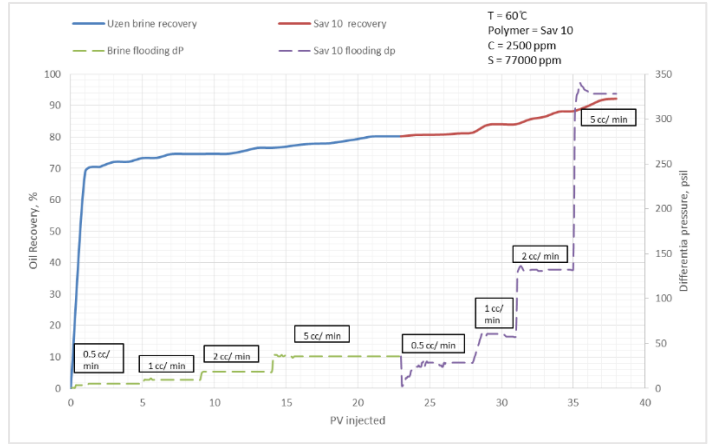


Figure 68 - Oil recovery of brine and polymer flooding and differential pressure as functions of injected pore volumes

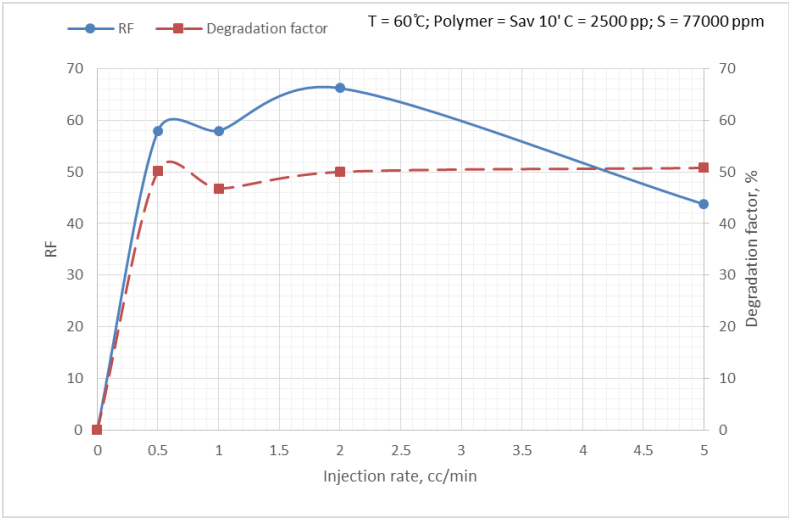


Figure 69 - Resistance and degradation factor as a function of injection rate

5. Conclusions and Recommendations

Different polymers were analyzed and based selection criteria, which were mentioned in the literature review and results section. The most suitable polymer for polymer flooding in the Uzen field was determined. The short outcomes of each experiment are provided below.

- Firstly, the bulk scale rheological investigation showed the effect of concentration and temperature alteration on rheology of three polymers. All polymers exhibited a shear-thinning behavior with an increase in shear rate. As for the effect of concentration and temperature, an increase in polymer concentration resulted in a rise in viscosifying ability of candidates, while elevated temperatures had the opposite effect.
- Mechanical stability of Sav 10 polymer was the highest one following by Sav 19 and Sav 10 XV stabilities. This is due to the difference in the molecular weights. Namely, Sav 10 has the lowest molecular weight.
- The result of long-term thermal stability test showed that all polymers can be stable at the temperature of 80 °C up to the time of writing (60 days).
- The injectivity of polymers to the sandstone core varied significantly for all three polymers. The more molecular weight of the polymer, the more pressure difference was required for the flooding. The main objectives of the experiment were to determine the mobility and permeability reduction during flooding of all solutions and pressure differences. Sav 10 demonstrated the best performance among other candidates and was chosen for the displacement test.
- Oil displacement test in the simulated conditions of the Uzen showed that application of polymer was effective and increased the cumulative oil recovery by almost 12 % after sufficient time of brine flooding.

Therefore, Sav 10 copolymer can be recommended as an appropriate candidate for the polymer flooding as tertiary recovery technique in the Uzen field.

The following are recommendations for future work:

- To get rock/fluid from samples the Uzen field. for more. This will allow to conduct deeper and more accurate laboratory investigation. For instance, rock samples with wider range of permeability (10-1200 mD), more variation of polymers and polymer concentration can be used in further works. A deeper investigation is required.
- To create sector simulation of polymer flooding with Sav 10 solution in the reservoir conditions of the Uzen field to evaluate its performance on the larger scale.

6. REFERENCES

- Algharaib, M., Alajmi, A., & Gharbi, R. 2014. Improving polymer flood performance in high salinity reservoirs. *Journal of Petroleum Science and Engineering*, 115, 17-23.
- Baijal, S. K. 1975, January 1. Interaction During Polymer Flooding. *Society of Petroleum Engineers*.
- Bluhm, T. L., Deslandes, Y., Marchessault, R. H., Pérez, S., & Rinaudo, M. 1982. Solid-state and solution conformation of scleroglucan. *Carbohydrate Research*, 100(1), 117-130.
- Carreau, P. J. 1972. "Rheological Equations from Molecular Network Theories." *Transactions of the Society of Rheology* 16 (1): 99–127.
- C & C Reservoirs. 2010. Former Soviet Union. Uzen Field South Mangyshlak Basin, Kazakhstan. *Field Evaluation Report*.
- Chang, H. L. 1978. Polymer flooding technology yesterday, today, and tomorrow. *Journal of Petroleum Technology*, 30(08), 1-113.
- Connan, J. 1984. Biodegradation of crude oils in reservoirs. In" Advances in petroleum geochemistry"(J. Brooks and DH Welte, eds.), Vol. 1.
- Firozjaini, A. M., Zargar, G., & Kazemzadeh, E. 2018. An investigation into polymer flooding in high temperature and high salinity oil reservoir using acrylamide based cationic co-polymer: experimental and numerical simulation. *Journal of Petroleum Exploration and Production Technology*, 9(2), 1485-1494.
- Firozjaini, A. M, Manshad, A. K., Zargar, G., & Mohammadi, A. H. 2019. An experimental investigation into enhanced oil recovery (EOR) by polymer flooding in sandstone reservoirs under high temperature and high salinity conditions using a combination of two synthetic polymers. *Petroleum & Coal*, 61(1).
- Greaves, B. L., Marshall, R. N., & Thompson, J. H. 1984, January. Hitts lake unit polymer project. In *SPE Annual Technical Conference and Exhibition*. Society of Petroleum Engineers.

Green, D. W., & Willhite, G. P. (1998). *Enhanced oil recovery* (Vol. 6, pp. 143-154). Richardson, TX: Henry L. Doherty Memorial Fund of AIME, Society of Petroleum Engineers.

Hincapie, R. E. 2016. Pore-Scale Investigation of the Viscoelastic Phenomenon during Enhanced Oil Recovery (EOR) Polymer Flooding through Porous Media. *Papierflieger Verlag GmbH*.

Irvine, R. R., Davidson, J. C., Edwards, S., Kingsbury, J., Park, H. J., & Tardiff, C. A. 2012, January. Case study of polymer flood pilot in a low permeability Mannville sand of the Western Canadian sedimentary basin using produced water for blending. In *SPE Improved Oil Recovery Symposium*. Society of Petroleum Engineers.

Jennings, R. R., Rogers, J. H., & West, T. J. 1971. Factors influencing mobility control by polymer solutions. *Journal of Petroleum Technology*, 23(03), 391-401.

Jensen, T., Kadhum, M., Kozlowicz, B., Sumner, E. S., Malsam, J., Muhammed, F., & Ravikiran, R. 2018, April. Chemical EOR Under Harsh Conditions: Scleroglucan As A Viable Commercial Solution. In *SPE Improved Oil Recovery Conference*. Society of Petroleum Engineers.

Levitt, D. B., Slaughter, W., Pope, G., & Jouenne, S. 2011a. The effect of redox potential and metal solubility on oxidative polymer degradation. *SPE Reservoir Evaluation & Engineering*, 14(03), 287-298.

Levitt, D. B., Pope, G. A., & Jouenne, S. 2011. Chemical degradation of polyacrylamide polymers under alkaline conditions. *SPE Reservoir Evaluation & Engineering*, 14(03), 281-286.

Li, Q., Pu, W., Wei, B., Jin, F., & Li, K. 2017. Static adsorption and dynamic retention of an anti-salinity polymer in low permeability sandstone core. *Journal of Applied Polymer Science*, 134(8).

Liang, K., Han, P., Chen, Q., Su, X., & Feng, Y. 2019. Comparative Study on Enhancing Oil Recovery under High Temperature and High Salinity: Polysaccharides Versus Synthetic Polymer. *ACS omega*, 4(6), 10620-10628.

Liu, H., Wang, Y., & Liu, Y. Z. 2006. Mixing and injection techniques of polymer solution. *Enhanced Oil Recovery–Polymer Flooding*, (Eds.: Y.-Z. Liu et al.), Petroleum Industry Press, Beijing, 157-181.

- Luo, J. H., Liu, Y. Z., & Zhu, P. 2006. Polymer solution properties and displacement mechanisms. *Enhanced Oil Recovery-Polymer Flooding; Shen, P.-P., Liu, Y.-Z., Liu, H.-R., Eds*, 1-72.
- Moradi-Araghi, A., & Doe, P. H. 1987. Hydrolysis and precipitation of polyacrylamides in hard brines at elevated temperatures. *SPE Reservoir Engineering*, 2(02), 189-198.
- Niu, J. G., Chen, P., Shao, Z. B., Wang, D. M., Sun, G., & Li, Y. 2006. Research and development of polymer enhanced oil recovery. *Research and development of enhanced oil recovery in Daqing. Petroleum Industry Press, Beijing*, 227-325.
- O'Leary, W. B., Boivin, J. W., Dasinger, B. L., Beck, D., Goldman, I. M., & Wernau, W. C. 1987. Biocide evaluation against sessile xanthan polymer-degrading bacteria. *SPE Reservoir Engineering*, 2(04), 647-652.
- Quadri, S. M. R., Shoaib, M., AlSumaiti, A. M., & Alhassan, S. M. 2015. Screening of polymers for EOR in high temperature, high salinity and carbonate reservoir conditions. In *International petroleum technology conference*. International Petroleum Technology Conference.
- Rellegadla, S., Prajapat, G., & Agrawal, A. 2017. Polymers for enhanced oil recovery: fundamentals and selection criteria. *Applied microbiology and biotechnology*, 101(11), 4387-4402.
- Rodrigues, N. 2012. Accounting for reservoir uncertainties in the design and optimization of chemical flooding processes. Master of Science in Engineering; University of Texas: Austin
- Salmo, I. C., Pettersen, Ø., & Skauge, A. 2017. Polymer flooding at an adverse mobility ratio: acceleration of oil production by crossflow into water channels. *Energy & Fuels*, 31(6), 5948-5958.
- Sandengen, K., Meldahl, M. M., Gjersvold, B., Molesworth, P., Gaillard, N., Braun, O., & Antignard, S. 2018. Long term stability of ATBS type polymers for enhanced oil recovery. *Journal of Petroleum Science and Engineering*, 169, 532-545.
- Seright, R. S., Adamski, R. P., Roffall, J. C., & Liauh, W. W. 1983, April. Rheology and mechanical degradation of EOR polymers. In *SPE/British Society of Rheology Conference on Rheology in Crude Oil Production*.

- Seright, R. S., Seheult, J. M., & Talashek, T. 2009. Injectivity characteristics of EOR polymers. *SPE Reservoir Evaluation & Engineering*, 12(05), 783-792. Seright, R. S., Campbell, A., Mozley, P., & Han, P. 2010. Stability of partially hydrolyzed polyacrylamides at elevated temperatures in the absence of divalent cations. *Spe Journal*, 15(02), 341-348.
- Seright, R. S., & Skjevrak, I. 2014, April. Effect of dissolved iron and oxygen on stability of HPAM Polymers. In *SPE Improved Oil Recovery Symposium*. Society of Petroleum Engineers.
- Sheng, J. J. 2011. *Modern Chemical Enhanced Oil Recovery: Theory and Practice*, first edition. Amsterdam: Elsevier.
- Sheng, J. J. 2014. A Comprehensive Review of Alkaline–Surfactant– Polymer (ASP) Flooding. *Asia-Pac J Chem Eng* 9 (4): 471–489. [http:// dx.doi.org/10.1002/apj.1824](http://dx.doi.org/10.1002/apj.1824).
- Sheng, J. J., Leonhardt, B., & Azri, N. 2015. Status of polymer-flooding technology. *Journal of Canadian Petroleum Technology*, 54(02), 116-126.
- Sorbie, K. S. 2013. *Polymer-improved oil recovery*. Springer Science & Business Media.
- Sparke, S. J., Kislyakov, P. Y., & Amirtayev, M. A. (2005, June). Significant Production Enhancement in Uzen Field, Kazakhstan through Surface and Subsurface Optimization (SPE94360). In *67th EAGE Conference & Exhibition* (pp. cp-1). European Association of Geoscientists & Engineers.
- Standnes, D. C., & Skjevrak, I. 2014. Literature review of implemented polymer field projects. *Journal of Petroleum Science and Engineering*, 122, 761-775.
- Taber, J. J., Martin, F. D., & Seright, R. S. 1997. EOR screening criteria revisited-Part 1: Introduction to screening criteria and enhanced recovery field projects. *SPE reservoir engineering*, 12(03), 189-198.
- Tan, Z.-L., 1998. HAPM thermal stability under reservoir conditions. In: Gang, Q.-L., et al. (Eds.), *Chemical Flooding Symposium—Research Results during the Eighth Five-Year Period (1991–1995)*, Vol. I. *Petroleum Industry Press*, pp. 107–111.
- Ulmishek, G. F. 1990. Uzen Field--USSR Middle Caspian Basin, South Mangyshlak Region.

- Vermolen, E., Van Haasterecht, M. J., Masalmeh, S. K., Faber, M. J., Boersma, D. M., & Gruenenfelder, M. A. 2011, January. Pushing the envelope for polymer flooding towards high-temperature and high-salinity reservoirs with polyacrylamide based ter-polymers. In *SPE middle east oil and gas show and conference*. Society of Petroleum Engineers.
- Wang, D., Xia, H., Liu, Z., & Yang, Q. 2001, January. Study of the mechanism of polymer solution with visco-elastic behavior increasing microscopic oil displacement efficiency and the forming of steady "Oil thread" flow channels. In *SPE Asia Pacific oil and gas conference and exhibition*. Society of Petroleum Engineers.
- Wang, G., Yi, X., Feng, X., Jing, B., & Ouyang, J. 2012. Synthesis and study of a new copolymer for polymer flooding in high-temperature, high-salinity reservoirs. *Chemistry and Technology of Fuels and Oils*, 48(2), 112-119.
- Wang, C., Liu, P., Wang, Y., Yuan, Z., & Xu, Z. 2018. Experimental Study of Key Effect Factors and Simulation on Oil Displacement Efficiency for a Novel Modified Polymer BD-HMHEC. *Scientific reports*, 8(1), 1-9.
- Wu, S. (2016). Rheological Properties of Viscoelastic Polymer Solutions (Doctoral dissertation).
- Yanbiao, Z. F. Y. G. L., & Jiangbo, L. 2005. Development of Chemical Oil Displacement Agent for High Temperature and High Salinity Reservoir [J]. *Advances in Fine Petrochemicals*, 5.
- Yang, S. H., & Treiber, L. E. 1985, January. Chemical stability of polyacrylamide under simulated field conditions. In *SPE Annual Technical Conference and Exhibition*. Society of Petroleum Engineers.
- Yang, F., Wang, D., Wang, G., Sui, X., Liu, W., & Kan, C. 2006, January. Study on high-concentration polymer flooding to further enhance oil recovery. In *SPE Annual Technical Conference and Exhibition*. Society of Petroleum Engineers.
- Zhang, Y., Wei, M., Bai, B., Yang, H., & Kang, W. 2016, April. Survey and data analysis of the pilot and field polymer flooding projects in China. In *SPE improved oil recovery conference*. Society of Petroleum Engineers.

